OPTIMIZATION OF THERMAL PERFORMANCE OF WATER IN GLASS EVACUATED TUBE SOLAR HEATER

KYEKYERE ERNEST

MASTER OF SCIENCE
(Mechanical Engineering)

PAN AFRICAN UNIVERSITY INSTITUTE
FOR BASIC SCIENCES, TECHNOLOGY
AND INNOVATION

2021

Optimization of Thermal Performance of Water in Glass Evacuated Tube Solar Heater

Kyekyere Ernest

A thesis submitted in partial fulfillment of the requirement for the degree of Master of Science in Mechanical Engineering in the Pan African University Institute for Basic Sciences, Technology and Innovation

2021

DECLARATION

This thesis is my original work and has not been presented for a degree award in this or any other university.

Sign..... Date.....

Kyekyere Ernest

This thesis has been submitted with our approval as supervisors:

Sign..... Date.....

Dr. Eng. Hiram Ndiritu

JKUAT, Kenya

Sign..... Date.....

Dr. Meshack Hawi

JKUAT, Kenya

DEDICATION

I dedicate this work to my beautiful wife Mwambe Polline and my entire family especially my Dad, Mr Ernest Okyere of blessed memory for their continuous support, encouragement and prayers.

ACKNOWLEDGEMENT

First and foremost, I would like to express my gratitude and appreciation to the Almighty God for His guidance and protection throughout this work. I also want to express my heartfelt gratitude and thanks to my supervisors, Dr. Eng. Hiram Ndiritu and Dr. Meshack Hawi for their guidance and invaluable support in this research work. I am grateful to Mr. Joseph Muigai and Mr. Tom Waka of J.K.U.A.T Thermodynamics and Fluid mechanics laboratories for their immense help in developing the experimental setup.

I am sincerely grateful to the administration and the staff of Pan African University Institute for Basic Sciences, Technology and Innovation (PAUSTI) for their immense support.

Finally, I want to specially thank my family and colleagues for their love and encouragement throughout the research period.

TABLE OF CONTENTS

LIST OF TABLES

LIST OF FIGURES

LIST OF APPENDICES

LIST OF ABBREVIATIONS

WG-ETSWH	Water in Glass Evacuated Tube Solar Water Heater
SWH	Solar Water Heater
CFD	Computational Fluid Dynamics
WG-ETSC	Water in Glass Evacuated Tube Solar Collector
UP-ETSC	U Pipe Evacuated Tube Solar Collector
LPG	Liquefied Petroleum Gas
FPSC	Flat Plate Solar Collector
ETSC	Evacuated Tube Solar Collector
FVM	Finite Volume Method
BA	Boussinesq Approximation
VPT	Variation of the Properties with Temperature
ANN	Artificial Neural Network
HTS	High-Throughput Screening
MOGA	Multi-Objective Genetic Algorithm

NOMENCLATURE

Symbols

A_c	Surface area of collector (m^2)
c_{pw}	Specific heat of water at constant pressure ($kJ/(kg^oK)$)
c_p	Specific heat capacity ($kJ/(kg^oK)$)
G	Solar irradiation
m	Mass of water (kg)
N	Number of data points
P	Pressure (Pa)
Q	Heat gain (MJ/m^2)
k	Thermal conductivity ($W/(m.K)$)
R_{VA}	Ratio of the storage tank volume to the collector area (L/m^2)
T_b	Temperature at bottom of the tank (^oC)
T_{in}	Initial temperature in the tank (^oC)
T_m	Temperature at middle of the tank (^oC)
T_{out}	Outlet temperature of the tank (^oC)
T_u	Temperature at upper portion of the tank (^oC)
T	Temperature (^oC)
t	Time (s)

u	Velocity (ms^{-1})
U	Uncertainty
V	Volume (m^3)
X_i	Position tensor

Greek Symbols

η	Efficiency of solar water heater
σ	Standard deviation
ρ_w	Density of water (kg/m^3)
ρ	Density (kg/m^3)
μ	Dynamic viscosity ($kg/m.s$)
δ	Change in parameter

Subscripts

a	Atmospheric
b	Bottom of tank
d	Daily
m	Middle portion of tank
u	Upper portion of the tank

ABSTRACT

Solar water heaters provide a cost-efficient, unlimited, and environmentally friendly approach to hot water generation. Water in glass evacuated tube solar water heater (WG-ETSWH) is one of the commonly used solar water heaters (SWHs) available in the market. Despite its widespread use, WG-ETSWH has a low thermal performance and its installation cost is very high. As a result, hot water generation in homes and industries is highly dependent on electricity, fossil fuels, and traditional biomass despite the high solar potential in Africa. That has resulted in environmental pollution, various health problems and the high cost of conventional fuels. Several research studies have been conducted to help improve the performance of water in glass evacuated tube solar collectors (WG-ETSC). The performance of WG-ETSWH is dependent on the geographic location. Additionally, for collectors with identical parameters, tilt-type collectors absorb slightly more solar irradiation than horizontal-type collectors. The optimum thickness of the polyurethane insulation to reduce heat loss from the storage tank is 50 mm. However, the effect of collector tube length, diameter and tilt angle on the performance of WG-ETSWH has not been fully studied. This research work is focused on optimizing the performance of WG-ETSWH for water heating applications using both experimental and numerical methods under the climatic conditions in Kenya. An experimental study on the performance of WG-ETSWH was conducted under the climatic conditions in Kenya. A CFD model was developed according to the specifications of the experimental setup and its performance was then validated against the experimental data. The validated CFD model was then used to study the influence of geometric variables such as the collector tilt angle, collector tube diameter and the collector tube length on the performance of the system. From the experimental study, the outlet temperature of the water in glass evacuated tube solar water heater was found to be ranged from 55 ^{o}C to 69 ^{o}C given an initial temperature of 25 ^{o}C for a whole day heat collection. The daily efficiency of the water in glass evacuated tube solar water heater under the climatic conditions in Kenya ranges from 58 % to 65 %. The collector tube length, diameter and tilt angle had a significant influence on the

performance of WG-ETSWH. The optimum collector tube length, diameter and tilt angle were found to 2000 mm, 50 mm and 28 degrees respectively. The optimized design of the WG-ETSWH enhanced the outlet temperature of the water in the storage tank by 6.0 % and the average flow velocity of water in the system by 11.8 %. The results from this research will give insight into the design of improved products of water in glass evacuated tube solar water heater for the extraction of maximum heat energy from the sun.

CHAPTER ONE

INTRODUCTION

1.1 Background

Population increase and technological advancement have led to a significant rise in energy demand worldwide (Kannan & Vakeesan, 2016). Global energy demand increased by an amount of 3% in 2018 relative to 2017 (Energy Analyis, 2019). In 2019, global primary energy consumption grew by 1.3% relative to 2018 (Energy Analyis, 2020). This has resulted in energy shortages which are of concern globally (Kyekyere et al., 2021). Fossil fuels have been used over the years to satisfy the energy demand of the world. In 2017, fossil fuels provided almost 80% of the world's energy demand (REN21, 2019). However, the fossil fuel reserves are progressively decreasing and getting exhausted (Armaroli & Balzani, 2007).

Additionally, the excessive usage of fossil fuels produce harmful emissions which leads to climate change, ozone layer depletion and causes various health problems to mankind. Fossil fuel usage results in the production of carbon dioxide (CO_2) which leads to global warming. In 2018, CO_2 emissions grew by 2.0% than in 2017 (Energy Analyis, 2019). Besides, emissions such as carbon monoxide (CO) and nitrogen oxides (NO_x) from the use of fossil fuel leads to environmental pollution and various health problems.

To preserve the environment and provide an unlimited energy supply for the future, it is vital to explore renewable energy sources. Renewable energy is cost-effective, reliable, and environmental friendly with little or no emissions (Alanne & Saari, 2006). Renewable resources of energy accounted for an overall 18.1% of global final energy consumption as of 2017, out of which modern renewables accounted for 10.6%, whereas traditional usage of biomass for cooking and heating in developing countries accounted for 7.5% (REN21, 2019).

Modern renewable energy sources include wind energy, solar energy, geothermal energy, and hydro power. However, the most accessible and freely available source of all clean energy options is solar energy (Panwar et al., 2011). It, therefore, has the capacity of being used to partially address the worlds growing energy demand.

There are numerous applications of solar energy; it can be converted directly to electricity using photovoltaic cells or converted to thermal energy for heating and cooling purposes using solar thermal collectors. At the close of 2016, heating and cooling contributed to about 51% of the total world energy usage of which modern renewable energy sources supplied only 10% of the demand (REN21, 2019).

Energy for heating and cooling is largely from fossil fuels and traditional biomass, generating nearly 40% of global CO_2 emissions (REN21, 2019). The effect of traditional biomass usage in heating applications is the destruction of forest and consequently desertification. The utilization of solar energy in heating and cooling applications could help preserve the environment and provide an unlimited energy supply for the future.

There is an increasing demand for energy in the household sector due to an increase in population. In 2018, the building sector accounted for about 30%

of the global energy usage, contributing to about 31% of energy-related CO_2 emissions (Global Alliance for Buildings and Construction, 2019). Household sector energy consumption involves usage for cooling, heating, ventilation, and hot water generation. Hot water generation accounts for a larger proportion of the household sector energy demand. Hot water generation accounts for about 30% - 40% of a family's electricity bill (Veeraboina & Ratnam, 2012). It is estimated that in Nairobi, electricity supplies 37% of the hot water demand while LPG supplies 24% of the demand (Momanyi, 2015).

Water is generally heated by burning non-commercial fuels, namely, firewood as in the rural areas and commercial fuels such as kerosene oil, Liquefied Petroleum Gas (LPG), coal, and electricity in urban areas (Lee & Sharma, 2007). Solar water heaters have the capacity of reducing environmental pollution resulting from the use of conventional fuels in water heating applications, reducing the cost of fuels and addressing the world's energy crisis (Kalogirou, 2004).

1.2 Solar Water Heaters

Solar water heaters are categorized as concentrating and non- concentrating collectors. Concentrating collectors use mirrors to concentrate the solar radiation while the non-concentrating collectors absorb the solar radiation without concentration. Non- concentrating solar collectors are classified as Flat Plate Solar Collectors (FPSCs) and Evacuated Tube Solar Collectors (ETSCs).

Evacuated tube collectors have better performance than flat-plate collectors for high-temperature operation because of reduced convection heat loss due to the vacuum envelope around the absorber surface (Budihardjo et al., 2007). Figure 1.1 illustrates various ways of harvesting solar energy.

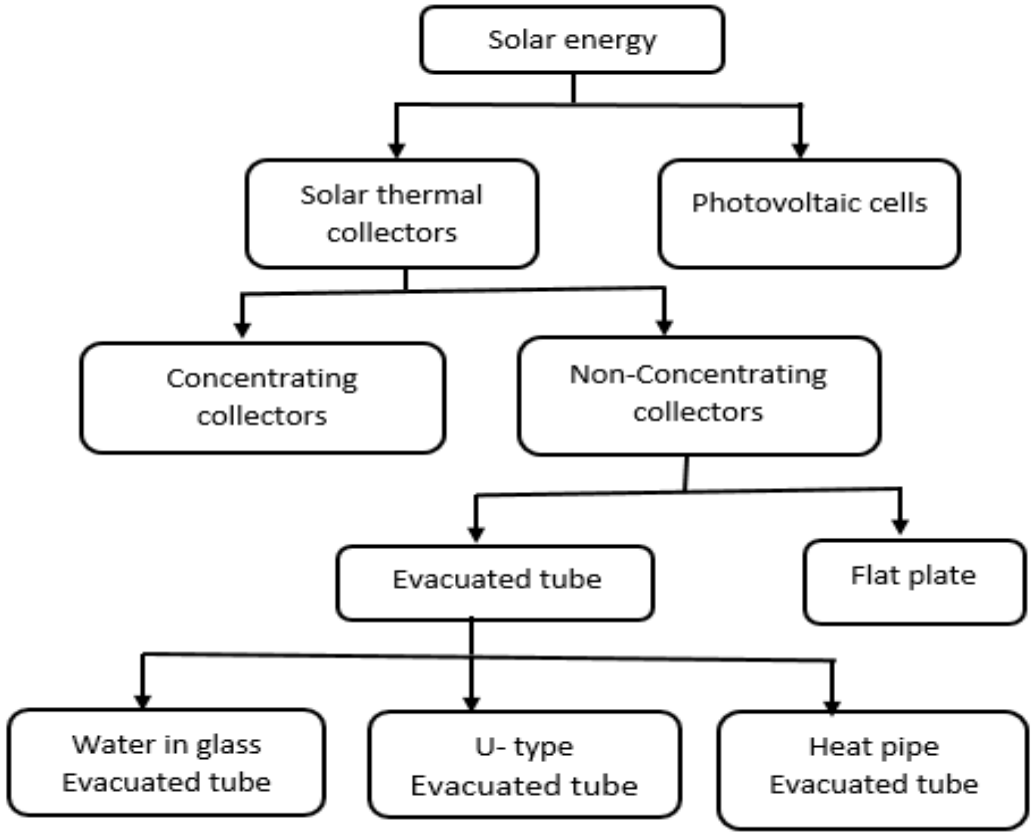

Figure 1.1: Solar Harvesting Techniques (Ali Omer Ali, 2019)

There are three types of Evacuated tube solar water heaters, namely: Water in glass evacuated tube solar heater, U-type evacuated tube solar water heater and heat pipe evacuated tube solar water heater. However, this research study focuses on water in glass evacuated tube solar water heater. The payback period of water in glass evacuated tube solar water heater is relatively short as compared to other types of evacuated tube solar water heaters. Hence, optimizing its performance will greatly enhance its competitiveness with fossil fuel, electricity and biomass in hot water generation.

The choice of water in glass evacuated tube solar water heater is due to its simple

design, cost effectiveness, longer life and its effectiveness in converting sunlight into heat.

Solar water heaters have the capacity of being used to address the world's thermal energy demand. It provides a carbon-free and sustainable supply of energy for heating applications thereby eliminating the harmful emissions resulting from the excessive use of fossil fuels and traditional biomass. The challenges of solar water heaters, however, is the high initial installation cost and its low efficiency in converting solar irradiation into thermal energy (Stryi-Hipp et al., 2012).

1.3 Problem Statement

Over the years, efforts have been made to utilize renewable energy sources in hot water generation. Solar thermal energy proves to be the most convenient source of energy for hot water generation through solar water heaters. Water in Glass Evacuated Tube Solar Collector(WG-ETSC) is the most commonly used solar water heater due to its simple design and low manufacturing cost (Budihardjo et al., 2007). It can therefore be utilized for small scale heating purposes. However, WG-ETSCs have low thermal performance. As a result, small scale heating applications in homes, dormitories, hotels, and industries are so much dependent on fossil fuels, electricity, and traditional biomass (charcoal, firewood, animal dung, and grass agricultural residue) in Africa (Kamau, 2013). This has resulted in harmful emissions which pollute the environment, causes various health problems and leads to global warming.

Improving the efficiency and performance of WG-ETSCs will enhance its utilization. This will help to reduce harmful emissions generated from the excessive use of fossil fuel and reduce the cost of conventional fuels. The performance of a

solar water heater is determined by the product configuration and the local meteorological conditions (Budihardjo & Morrison, 2009). Various parameters such as the tilt angle, the weather conditions, the collector dimensions may affect the overall performance of the water in glass evacuated tube solar collectors (Hayek, 2009).

Several research studies have been conducted to help improve the performance of WG-ETSC. However, effect of collector tilt angle, length and diameter on the performance of WG-ETSC have not been fully studied. A need, therefore, arises to investigate the effect of these geometric parameters on the performance of water in glass evacuated tube solar collectors.

1.4 Objectives

1.4.1 Main Objective

The main objective of this research is to optimize the thermal performance of water-in-glass evacuated tube solar collectors. This will be achieved via the following specific objectives.

1.4.2 Specific Objectives

1. To evaluate through experimental measurements, the performance of water in glass evacuated tube solar water heater used in Kenyan climatic conditions.

2. To develop and validate a CFD model of the water in glass evacuated tube solar water heater for simulation of its performance in Kenya.

3. To test the influence of geometric and flow variables through simulation to predict off-design performance of the system.

4. To optimize the performance of water in glass evacuated tube solar water heater through simulation.

1.5 Justification

The rise in global demand for energy has drawn the attention of researchers to explore various renewable sources of energy. Conventional sources of energy have been used over the years to meet the growing energy demand. However, the gradual depletion and the negative effects associated with the continuous usage of fossil fuels poses a threat to humanity and the environment.

Utilization of solar energy in hot water generation through the use of solar water heaters has the potential to reduce the demand for fossil fuels and the environmental pollution resulting from the use of the fossil fuels. However, the thermal performance and the initial installation cost of solar water heaters are limitations to its usage. Improving the performance of water in glass evacuated tube solar water heater will enhance its utilization. This will increase its competitiveness with conventional energy sources helping to reduce the negative impact associated with the use of conventional fuels.

This research focuses on the study and optimization of the thermal performance of water in glass evacuated tube solar water heater for domestic hot water generation.

1.6 Scope of Research

The focus of this research study was to optimize the thermal performance of water in glass evacuated tube solar water heater. An experimental investigation of the performance of the WG-ETSWH was conducted during the months of

January and February 2021 and a CFD model developed using the specifications of the experimental setup. Numerical simulations were conducted to predict the performance of the WG-ETSWH using ANSYS Fluent software. Results from the numerical simulation were compared with data from experimental measurements to ascertain the validity of the CFD model.

The validated CFD model was then used to test the influence of geometric parameters on the performance of the water in glass evacuated tube solar water heater. Geometric parameters considered include the collector tube tilt angle, diameter of collector tube and the length of the collector tube. These geometric parameters were optimized to enhance the performance of the WG-ETSWH using ANSYS Design Explorer.

1.7 Thesis Outline

This thesis contains five chapters. The first chapter is the introduction which provides information on the current global energy demand, challenges and the importance of this research. It is categorized into background, problem statement, research objectives, justification and scope of the research. Literature review is the second chapter of this thesis and it presents studies conducted by other researchers to improve the performance of WG-ETSWHs. The chapter also highlights the findings of the researchers and the research gaps that need to be addressed.

In the third chapter, the methodology used for the study is presented. It includes the description of the experimental setup, experimental methods, instrumentation, performance analysis, design and sizing of the CFD model, simulation processes, validation of the CFD model and performance testing parameters. The

fourth chapter is results and discussion where data collected experimentally and numerically are analyzed and discussed. The final chapter is the conclusion and recommendations and it summarizes the findings and recommend necessary areas for further research study.

1.8 Journal Publication of Research

The first journal paper titled " The Performance of Water in Glass Evacuated Tube Solar Water Heater Under Kenya Climatic Condition" which was based on experimental data has been published in Computational Water, Energy and Environmental Engineering journal. The second article which covers the simulation aspects of the study is currently under preparation.

CHAPTER TWO

LITERATURE REVIEW

2.1 Overview

Solar thermal collectors convert solar radiation into thermal energy. The thermal energy produced can be used for heating and cooling purposes. Generally, solar thermal collectors are grouped into two; concentrating solar collectors and non-concentrating collectors. In concentrating solar collectors, mirrors and lenses are used to converge the sunlight radiation unto a particular area while solar radiation is not concentrated but absorbed directly in non-concentrating solar collectors.

2.1.1 Non-Concentrating Solar Collectors

There are two types of non-concentrating solar collectors, the evacuated tube solar collectors and flat plate solar collectors. Evacuated tube solar collectors generally have a better performance than flat plate solar collectors (Budihardjo et al., 2007).

2.1.2 Flat Plate Solar Collectors (FPSC)

Flat plate solar collector absorbs solar radiation from the sunlight and the heat energy absorbed is used to heat water for household use (bathing, washing among others). A FPSC system consists of a large copper or aluminium heat absorbing

plate soldered or bonded directly to copper pipes called risers, a glazing sheet, a layer of insulation, fluid channel, and a housing box. Figure 2.1 shows the pictorial view of the FPSC while Figure 2.2 shows the cross-section of the flat plate solar collector.

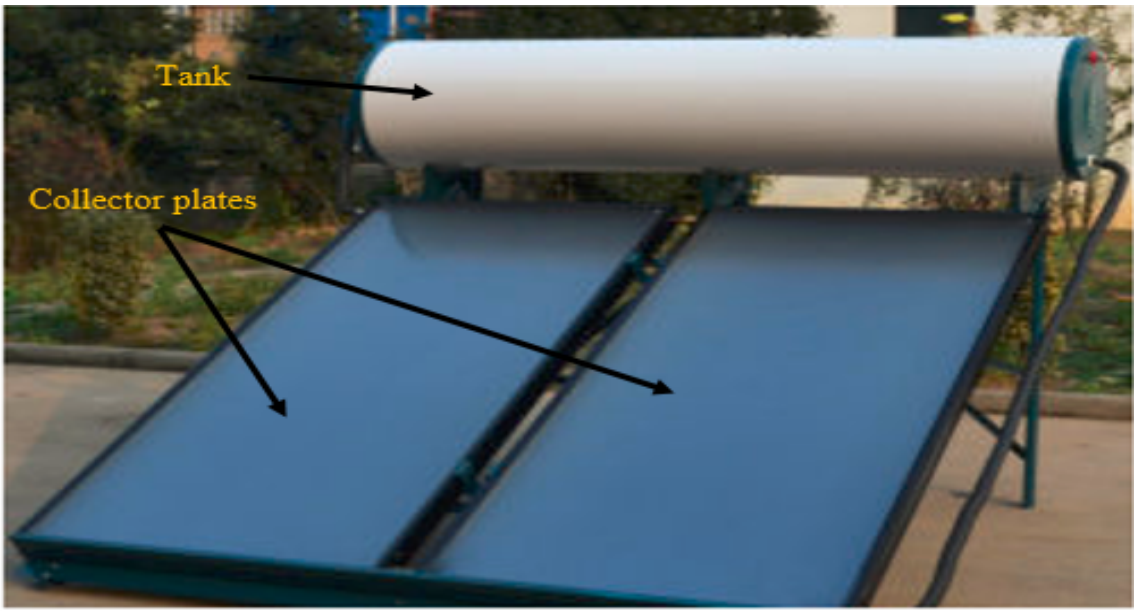

Figure 2.1: Pictorial View of FPSC (ESCO, 2015)

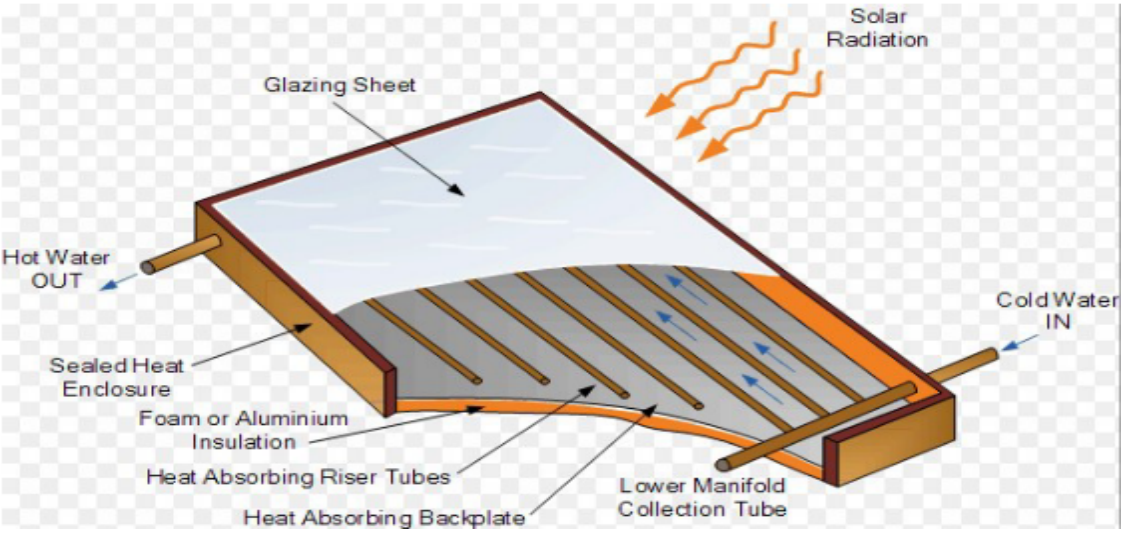

Figure 2.2: Cross-Section of FPSC (Ali Omer Ali, 2019)

2.1.3 Evacuated Tube Solar Collectors (ETSC)

Evacuated tube solar collectors are classified into three main groups, namely; water in glass evacuated tube solar collector, u-type evacuated tube solar collector and heat pipe evacuated tube solar collector (Alfaro-Ayala et al., 2015).

Water in glass and heat-pipe evacuated tube solar collectors are the two commonly used designs. However, water in glass evacuated tube solar collector is used widely due to its simple design and cost-effectiveness (Budihardjo & Morrison, 2009).

Heat-pipe evacuated tube solar water heaters consist of an evacuated tube and a heat pipe. The evacuated tube absorbs the solar radiations and converts it to thermal energy. The thermal energy is then transferred to a refrigerant inside the heat pipe, it vaporizes and rises rapidly into the condenser of the heat pipe where energy is transferred to the cold water. There is no direct connection between the refrigerant in the heat pipe and the water being heated. The thermal efficiency of heat-pipe evacuated tube solar collector is slightly higher than water in glass evacuated tube solar collector. However, the initial cost of a heat-pipe evacuated tube solar water heater is high and its payback period is long.

The u-type evacuated tube solar collector consist of an outer glass tube, an absorber tube and a u-shaped pipe. Between the outer glass tube and the absorber surface is a vacuum space to reduce heat loss. The u-pipe is coupled to a copper fin which is directly in contact with the absorber tube. The copper fin transmit heat from the absorber tube to the u-pipe which heats the working fluid in the u-pipe. Cold fluid entering one end of the u-pipe pushes hot fluid inside the u-

pipe up to the other end. There is a limited usage of u-type evacuated tube solar collector due its complex design and operating principles. Figure 2.3 and Figure 2.4 show the cross-sectional view of u-type and heat-pipe evacuated tube solar collectors respectively.

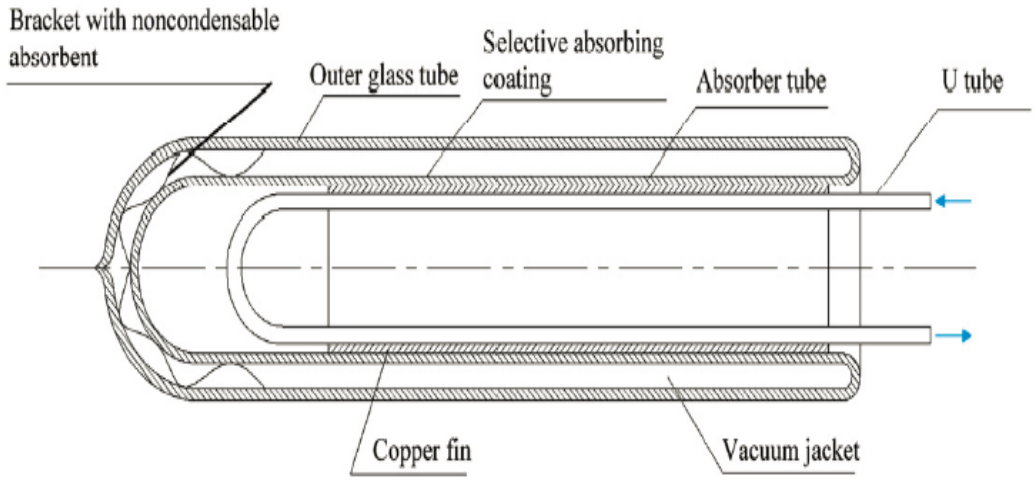

Figure 2.3: Cross Section of U-type Evacuated Tube Solar Collector (Ma et al., 2010)

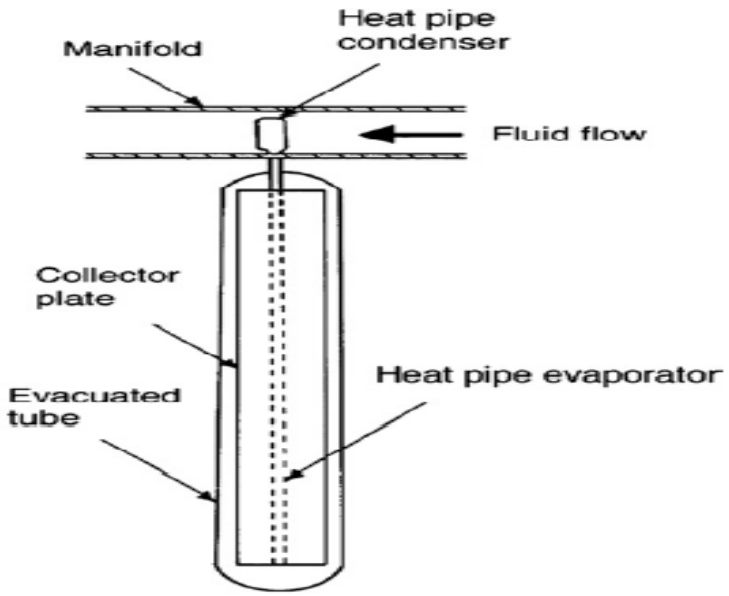

Figure 2.4: Cross Section of Heat-pipe Evacuated Tube Solar Collector (Ayompe & Duffy, 2013)

2.1.4 Water in Glass Evacuated Tube Solar Water Heater

The water in glass evacuated tube solar water heater (WG-ETSWH) is used for transforming solar radiation to thermal energy for heating applications. The basic parts of the WG-ETSWH system include the absorber surface, vacuum envelope, storage tank, fluid channel, and glass cover. Figure 2.5 shows the parts of the WG-ETSC system.

A WG-ETSWH consists of a set of single-ended glass tubes connected directly to a horizontally mounted storage tank. Each tube consists of an outer glass tube, which is transparent and bigger in diameter and an inner glass tube of smaller diameter. The outer surface of the inner glass tube is selectively coated (commonly with black enamel paint) for the absorption of solar radiations. A vacuum is created between the outer glass tube and the inner glass tube to reduce heat loss. An insulation layer is placed in between the walls of the storage tank to minimize heat loss.

Water flows from the tank to the tubes where it is heated by solar radiation. The heated water rises back to the storage tank and is replaced by cold water from the tank. Natural circulation of water purely drives the transfer of heat in the collector (Budihardjo et al., 2007).

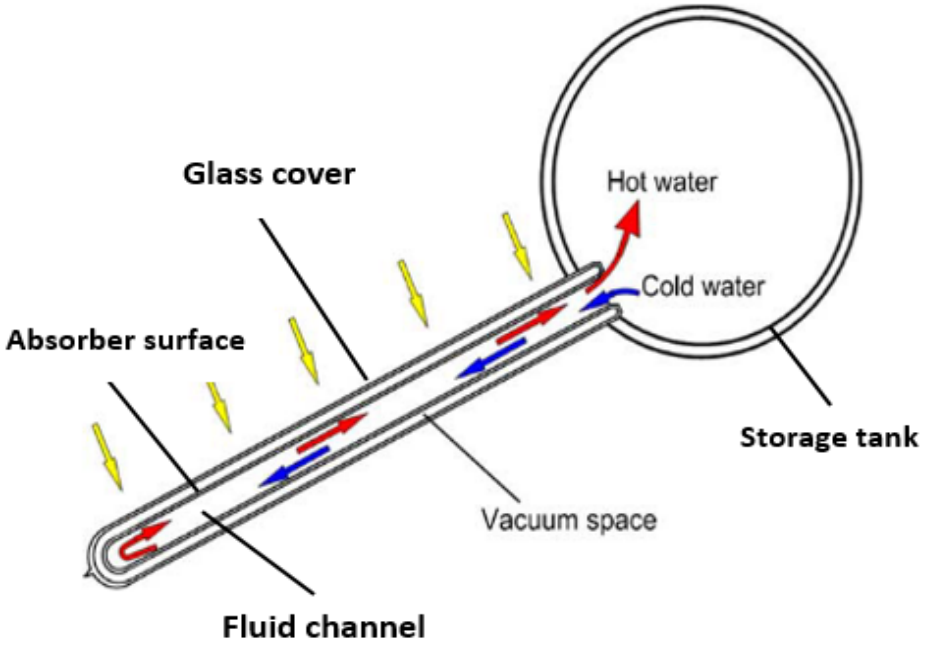

Figure 2.5: Cross Section of Water in Glass Evacuated Tube Solar Collector (Morrison et al., 2004)

2.2 Simulation of Performance of Water in Glass ETSC

Alfaro-Ayala et al. (2015) used CFD simulation in commercial ANSYS-Fluent software to study the thermal and hydraulic performance of water-in-glass evacuated tube solar collector, using the Finite Volume Method (FVM). They used 36 evacuated tubes constructed of borosilicate glass directly attached to a manifold and a steady-state laminar solver. The Boussinesq Approximation (BA) and the Variation of the Properties with Temperature (VPT) models were used and they found that the Boussinesq approximation is a more robust model for simulating the performance of low-temperature water-in-glass evacuated tube solar collectors.

Hayek (2009) investigated the characteristics of water-in-glass evacuated-tube solar collectors using advanced computational fluid dynamics (CFD) approaches. The author used turbulence models with different algorithms to handle the pressure-velocity coupling and several differencing schemes to discretize the convective transport terms. He concluded from the simulation that the glass tube should be made shorter and its length should be a function of the inclination angle of the entire collector.

Yao et al. (2015) investigated the performance of a solar water heater with twist tape inserts using CFD and compared the results with normal evacuated tubes solar collectors. They assumed the flow in the whole computational domain as laminar and neglected the heat conduction in the twisted tape. They concluded that for the twist tape inserts, water mixture near the top and bottom are more intense, disrupting the organized flow, and generates more eddy, making the temperature field more uniform. The twist tape inserts are ideal for relatively high-temperature heat transfer.

Morrison et al. (2005) used CFD package, ANSYS Fluent 6 (2001) to simulate the heat transfer and fluid flow in the collector tubes. They focused on the correlation for natural circulation rate through a single-ended tube mounted over a diffuse flat reflector inclined at 45 degrees. A constant pressure boundary condition on the open end was assumed. They concluded that the circulation flow rate through the tubes is influenced by two factors, namely the radiation intensity falling onto the absorber surface and the temperature of the storage tank.

Sato et al. (2012) investigated the fluid behavior in the tank of water in glass evacuated tube solar water heater using CFD models. They modified the convectional

collector by attaching lateral connections. The lateral connections increased the turbulence in the tank, reducing the region of stagnation in the storage tank. However, the performance of the system was compromised.

Budihardjo et al. (2003) used the transient simulation software, TRNSYS to test the performance of water-in-glass evacuated tube solar water heater. In the experiment, 21 water-in-glass evacuated tubes mounted at 45 degrees inclination coupled to a 150-litre horizontal tank was used. The results showed that the evacuated tube pre-heater system gives a 45% annual energy saving in Sydney. Evaluation of the cost-benefit of using solar water heaters in different regions is essential in increasing its patronage.

Ayompe et al. (2011) used the transient simulation software, TRNSYS to compare the performance of forced convection flat plate solar collector and evacuated tube solar collector. Their model predicted the collector outlet fluid temperature with percentage mean absolute error (PMAE) of 16.9% and 18.4% for the FPSC and ETSC systems, respectively.

Mohammadkarim et al. (2014) investigated the performance of evacuated tube solar collectors with natural circulation under the climatic conditions in Tehran city using TRNSYS software. Their results showed that the difference between useful energy gain and solar radiation on tilted surface during the summer season is less than that of the winter season, which renders the heat loss to be less than the winter season. Furthermore, in warm months the collector instantaneous efficiency and outlet temperature is greater than in cold months.

The evaluation of the simulation tools showed that CFD simulation using ANSYS Fluent can effectively be used to predict the performance of water in glass

evacuated tube solar collectors (WG-ETSCs). In the simulation, the equations governing the physical model are solved together with its surrounding conditions. Other simulation tools solve a limited number of equations (Ali Omer Ali, 2019). Table 2.1 shows the strength and weakness of the simulation tools.

Table 2.1: Weakness and Strength of ETSC Simulation Tools

Author	**Method**	**Strength**	**Weakness**
Alfaro-Ayala et al. (2015) Hayek (2009) Yao et al. (2015) Morrison et al. (2005)	CFD (ANSYS)	Governing equations are solved together with the environmental conditions	Complex and requires large computational space
Budihardjo et al. (2003) Ayompe et al. (2011) Mohammadkarim et al. (2014)	TRNSYS	Can be used to simulate and predict long term performance of ETSC	Solves limited number of equations

2.3 Optimization of Water in Glass ETSC

Zhang et al. (2014) tested the performance of more than 1000 sets of solar water heaters (SWHs), most of which were water-in-glass evacuated tube systems without reflectors in China. The experimental results showed that the heat gain from the sun and heat loss from the storage tank affected the thermal performance of SWHs. Their results predicted the optimum thickness of the polyurethane insulation to be 50 mm thick. Critical radius of insulation, a function of the thermal conductivity of the insulation material and the external convective heat transfer

coefficient is key in insulation thickness determination. Increasing the thickness of the insulation material to a value higher than the critical radius of insulation results in an increase in the rate of heat loss.

Morrison et al. (2004) did a preliminary investigation of the performance of very long water in glass evacuated tube solar collectors (greater than 2.4 m) and from the results, they concluded that very long tubes have the possibility of a stagnant region at the bottom of the tube that can affect its performance. However, the effect of stagnation region on the performance of the system and the optimum length of the collector were not fully explored.

Bracamonte et al. (2015) studied the effect of the tilt angle on flow patterns, energy conversion efficiency, and the stratification effect of water in glass evacuated tube solar water heater (ETSWH) in Venezuela. Tilt angles of 10 and 45 degrees were considered in the study. They reported that the tilt angle of the tube has a significant effect on the solar energy gain and flow patterns inside the storage tank. They concluded that lower tilt angles were preferable in such geographic location since lower tilt angles produced significantly higher temperatures. For any geographic location, water in glass evacuated tube solar water heater should be tilted such that the solar heat gain is maximized.

Tang et al. (2009) researched on how the use of Diffuse Flat Reflector (DFR) affect the performance of all-glass evacuated tubes. The result showed that the use of DFR can significantly increase the annual collectable radiation of a collector. They also compared the performance of tilt collectors and horizontal collectors of evacuated tubes. They found out that for collectors with identical parameters, tilt-type collectors absorb slightly more radiation than horizontal-type collectors.

2.4 Effect of Design Parameters on Performance of Water in Glass ESTC

Liu et al. (2017) successfully used a high-throughput screening (HTS) method based on an artificial neural network (ANN) model for the design of water in glass SWHs. The results of the study showed that the ANN-based HTS method can effectively predict the heat collection rates of water in glass evacuated tube solar water heaters. The artificial neural network is commonly used in forecasting and data classification. HTS method uses artificial intelligence to perform millions of computational tests.

Morrison et al. (2004) investigated the performance of a solar water heater with twist tape inserts and compared it with the normal one using CFD. They assumed the flow in the whole computational domain as laminar and neglected the heat conduction in the twisted tape. They concluded that, for twist tape inserts, water mixture near the top and bottom are more intense destroying the orderly flow and generates more eddy, making the temperature field more uniform. The twist tape inserts are suitable for heat transfer at relatively high temperatures.

Shah & Furbo (2007) investigated the effect of collector design using all glass evacuated tubular collector with horizontal tubes and employing computational fluid dynamics. Propylene-glycol/water mixture was used as the working fluid in the all glass evacuated tubular collector. In the experiment, collector tube lengths of 0.59 m, 1.17 m and 1.47 m were used for the study. They concluded that the collector tube with the shortest tube length of 0.59 m achieved the lowest average temperature.

2.5 Performance of Water in Glass SWH

Hayek et al. (2011) investigated the overall performance of water-in-glass tube and the heat-pipe solar collectors under local weather conditions as encountered along the Eastern coast of the Mediterranean Sea. Their results showed that the heat pipe solar collectors are better and its efficiency is about 15 to 20% higher than the water in glass solar collectors. However, the payback period for a heat-pipe collector is long.

Budihardjo & Morrison (2009) investigated the performance of water in glass evacuated tube solar collector systems and flat plate solar collectors in a range of locations using experimental measurements and a simulation model. It was revealed that the performance of two flat plate arrays with a collector area of 3.7 m^2 for domestic heating was higher than 30 evacuated tube arrays with a collector area of 2.9 m^2. This can be attributed to the difference in the collector area between the flat plate and the evacuated tube. The collector area is a key parameter in determining the quantity of solar radiation that can be absorbed.

Gao et al. (2013) compared the performance of water in glass evacuated tube solar collectors (WG-ETSCs) and U-pipe evacuated-tube solar collectors (UP-ETSCs) in Beijing. They concluded that the optimized mass flow rate for WG-ETSC and UP-ETSC applications is about 20–60 kg/hm^2 and 20–40 kg/hm^2 respectively in Beijing. Also, a higher flow rate reduces the energy collection of the water in the system.

Tang et al. (2011) compared the performance of water in glass ETSWH placed at tilt angles of 22 and 46 degrees, respectively, in China. Their results showed that

the collector tilt-angle of SWH had a significant influence on the daily collectable radiation and daily solar heat gain of a system. They concluded that to maximize the heat gain of solar water heaters, the collector should be inclined at a suitable tilt-angle dependent on the geographic location, for maximum absorption of solar radiation. The inclination of the tilt angle for maximum heat extraction is dependent on the geographic location.

2.6 Summary of Gaps

From the foregoing review of previous studies by different researchers on water in glass evacuated tube solar water heaters, some gaps were identified and are outlined as follows:

1. The performance of water in glass evacuated tube solar collector depends on the geographic location. The performance of water in glass ETSWHs needs to be investigated in Kenya.

2. The collector tilt angle has a significant influence on the solar energy gain and the flow patterns inside the storage tank. Multiple tilt angles need to be explored to determine the tilt angle for optimum performance.

3. Collector tube length and collector tube diameter affect the thermal performance of WG-ETSWH. Different collector tube lengths and diameters should be experimented to find out the optimum length and the optimum diameter.

4. The solar radiation absorption rate can be enhanced by the use of a solar tracker system. Research can be done in this area to improve the solar energy gain by the collector. However, in this research work emphasis will

not be placed in this area.

CHAPTER THREE

METHODOLOGY

3.1 Overview

The methodology used for conducting the performance testing of water in glass evacuated tube solar water heater (WG-ETSWH) via experimental measurements and CFD simulation is presented in this chapter. Experimental investigations were conducted to determine the performance of WG-ETSWH under the climatic conditions in Kenya followed by optimization of the system through CFD analysis.

A 3-D CFD model of the WG-ETSWH was developed in Inventor 2020 and imported into ANSYS simulation software for mesh development and simulation. ANSYS Fluent 18.1 was used to simulate the performance of the WG-ETSWH. The CFD model was validated against experimental data to ascertain that the model can predict the performance of the actual system with acceptable error margin. The validated numerical model was then used to test the influence of geometric and flow variables on the performance of the system. The procedures and techniques used in both experimental measurements and CFD simulations are described in this chapter. Figure 3.1 is a flow chart showing the outline of the study.

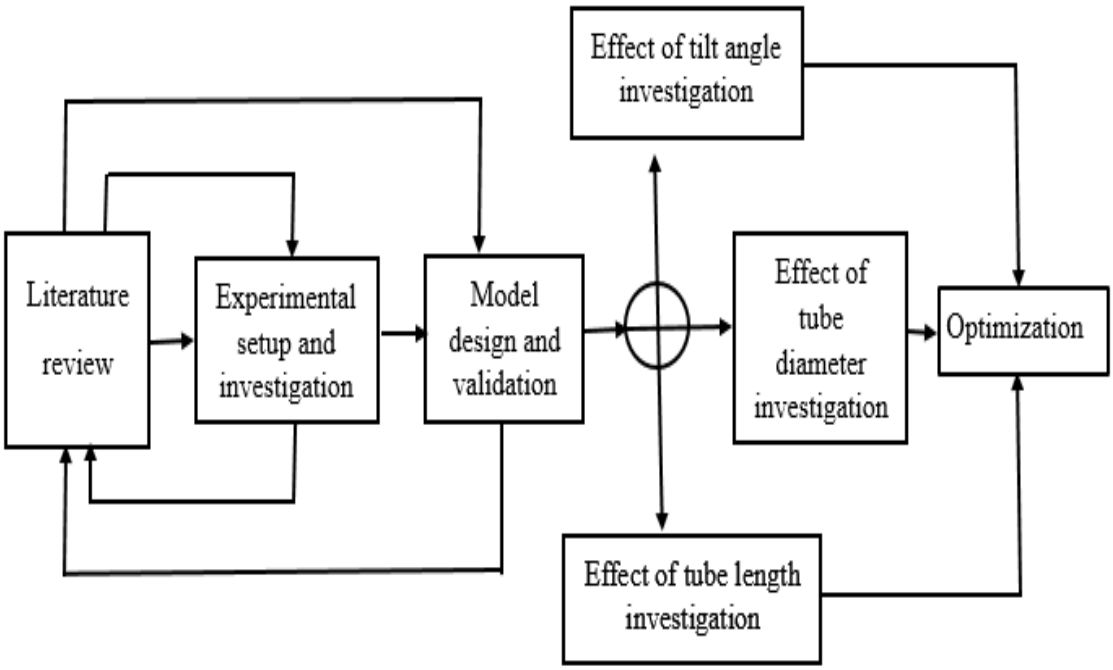

Figure 3.1: Flow Chart of the Study

3.2 Experimental Setup

3.2.1 Description of the Experimental Setup

An experimental set-up of the water in glass evacuated tube solar water heater was installed at an open area where maximum absorption of solar radiation could be obtained. The set-up consists of 20 evacuated tubes directly connected to a storage tank of 200-litre capacity. Each tube has a volume of 2.5 litre. The storage tank is made of a stainless steel inner cylinder and an insulated external casing. The insulation material is polyurethane and it has a thermal conductivity of about 0.022 W/(mk) at a temperature of 300 K (Engineering Toolbox, 2007).

Figure 3.2 shows the complete drawing of the experimental setup while Figure 3.3 shows the pictorial view of the experimental set-up of the evacuated tube solar

water heater.

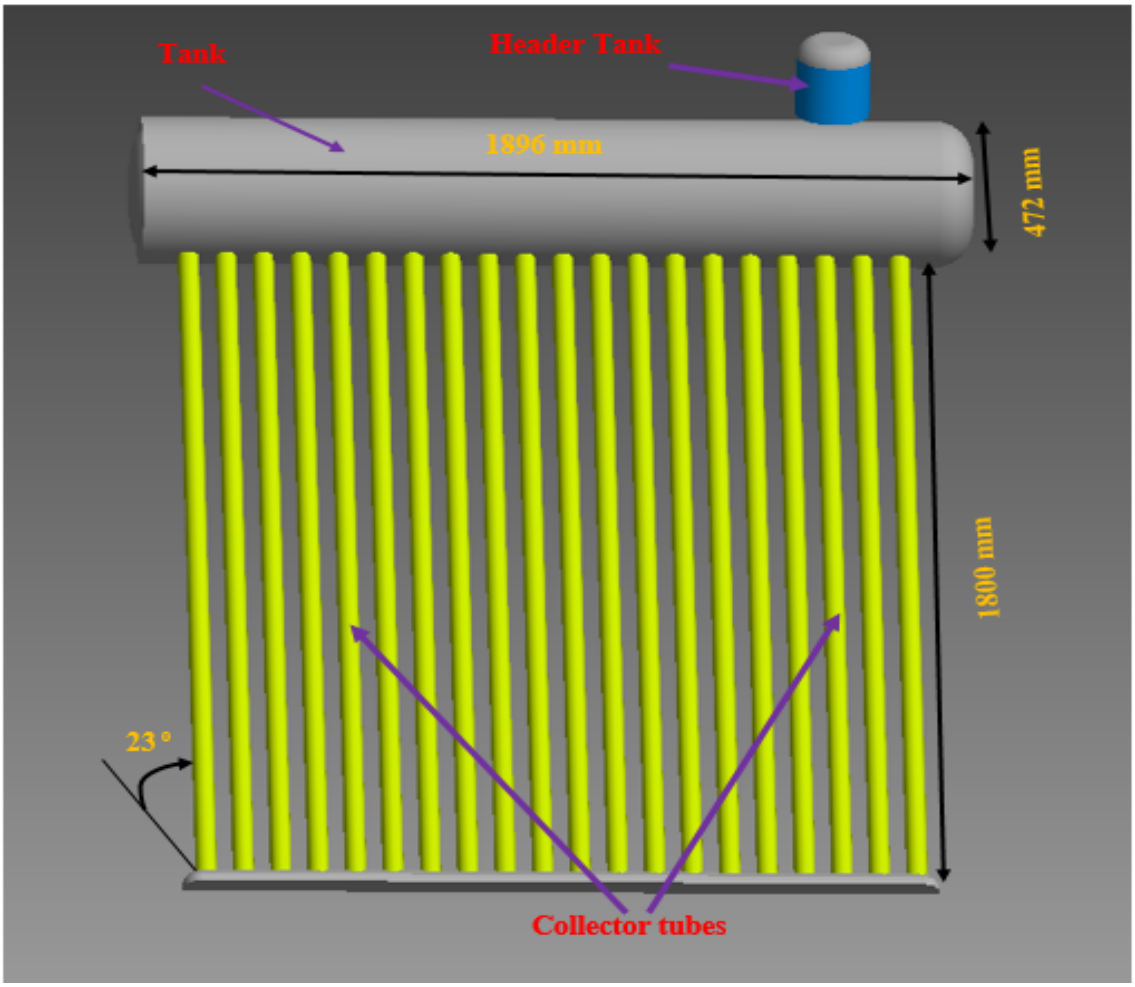

Figure 3.2: Experimental Set-up of WG-SWH

Attached to the main storage tank is a cold water header tank of capacity 8 litre. The supply of water to the system is through the cold water header tank which regulates the pressure in the system due to the limited pressure capacity of the evacuated tubes. The system operates at a maximum temperature of 200 ^{o}C and the evacuated tubes operate at a maximum pressure of 0.1 bar.

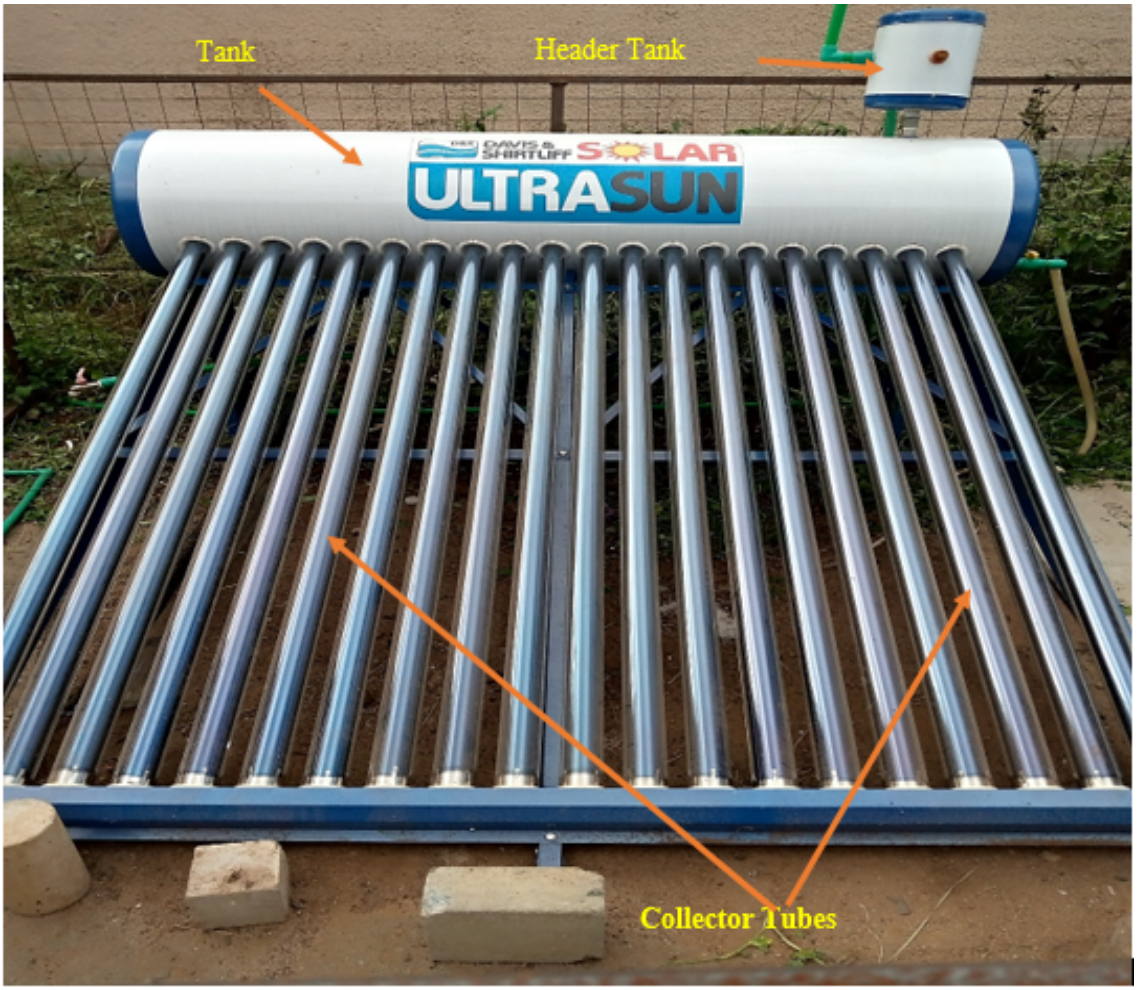

Figure 3.3: Pictorial View of the Experimental Set-up of WG-SWH

Water in glass evacuated tube solar water heaters are referred to as non- pressurized solar water heaters since it operates at very low pressure and does not require a pump to circulate the water. Evacuated tubes were inclined at an angle of 23 degrees to the horizontal as set by the supplier. Figure 3.4 shows the inner glass tube of smaller diameter selectively coated for absorption of solar radiation within the evacuated tube.

Specifications of the solar water heater are shown in Table 3.1. These specifications were chosen based on the current trend of water in glass evacuated tube

Figure 3.4: Coated Inner Tube Responsible for Solar Absorption

solar water heaters available in the Kenyan market and their installation angles.

Table 3.1: Specifications of the Solar Water Heater

S/No	Element	Specification
1	Tank volume	200 litres
2	Tank outer diameter	472 mm
3	Tank insulation thickness	48 mm
4	Length of tank	1896 mm
5	Outer tube diameter	58 mm
6	Inner tube diameter	47 mm
7	Tube length	1800 mm
8	Tube tilt angle	23 degrees
9	Absorber Area	3.28 m^2
10	Total volume of tubes	50 litres

3.2.2 Experimental Method

The two common methods used for testing the performance of solar water heaters are the water draw-off and the mixing water methods (Zhang et al., 2014). However, the water draw-off method is suitable for systems that operate at very high pressures. For a water in glass evacuated tube solar water heater, an appreciable volume of hot water is retained in the evacuated tubes when the draw-off method is used which could result in overestimation of the thermal performance of the system (Zhang et al., 2014). This makes the draw-off method unsuitable for performance testing of water in glass evacuated tube solar water heater.

The mixing water method was used in this study where the system was allowed to operate for 22 hours without drawing water from it. After the 22 hours, as hot

water in the system was drained through a drain valve located at the bottom of the storage tank, cold water was fed into the system simultaneously through the header tank until a uniform temperature of 27 $\pm$ 2 ^{o}C was obtained.

3.2.3 Data Measurement

The system was allowed to operate for 22 hours without drawing water from it. The ambient temperature, solar irradiation, wind speed and temperatures at points within the tank were measured on an hourly basis starting from 9:00 am in the morning to 5:00 pm in the evening.

The hot water was retained in the system till 7:00 am the next morning when the temperatures were measured to determine the amount of cooling during the night. An air vent located on the cold water header tank allowed air and vapour released inside the storage tank to be discharged.

3.2.4 Points of Temperature Measurement in the Tank

Daily measurements were taken from 9:00 am to 5:00 pm. Temperatures at different points in the tank as shown in Figure 3.5 were measured. The temperatures were measured inside the tank by inserting the digital thermometer through the holes located in Figure 3.5. The thermometers were about 30 mm deep in the storage tank at the time measurements were taken.

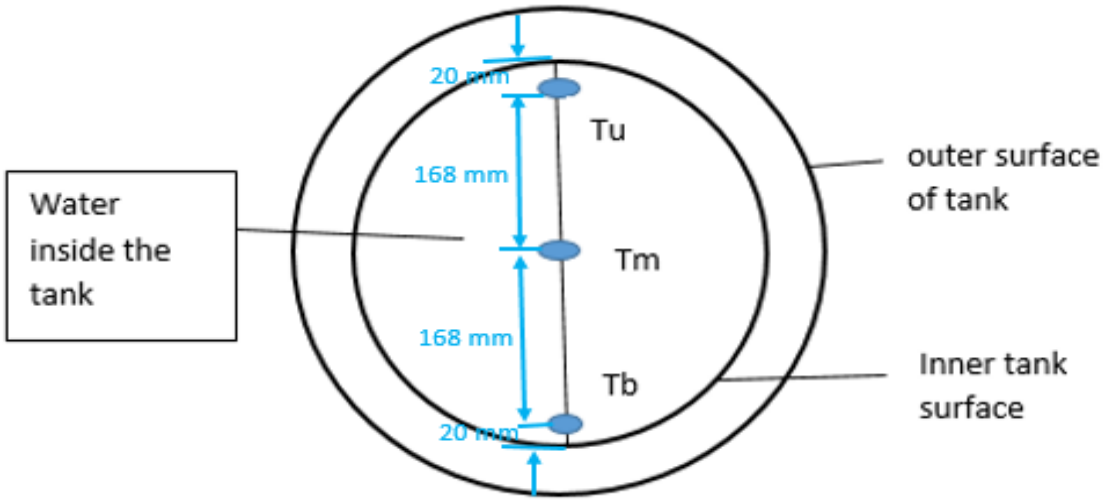

Figure 3.5: Points of Temperature Measurement in the Storage Tank

where T_u is the temperature at the topmost part of the storage tank, T_m is the temperature at the middle and T_b temperature at bottom of the storage tank.

3.2.5 Experimental Conditions

The experiments were conducted in an open area within Jomo Kenyatta University of Agriculture and Technology located in Juja, Kenya. The site has a latitude of 1.09 ^{o}S, a longitude of 37.0 ^{o}E and an altitude of 1.4 Km above sea level and it is mostly sunny throughout the year (Dindi, 2013). The study was conducted in the months of January and February, 2021.

The surrounding air temperatures ranged from 21 ^{o}C to 32 ^{o}C with an average ambient temperature of about 28 ^{o}C. The speed of wind in the surrounding measured during the study ranged from 0.5 m/s to 4 m/s with an average wind speed of 2.4 m/s while the solar irradiation in the area measured during the study ranged from 0 W/m^2 to 1100 W/m^2.

3.2.6 Instrumentation

Solar irradiation was measured using solar power meter TM- 206, the temperature readings in the tank were taken using digital thermometer type K(CA), weather station temperature and humidity sensor was used to measure atmospheric temperature while the speed of the wind was measured using anemometer. Table 3.2 shows specifications of the devices used for the data collection.

Table 3.2: Specification of the Measuring Devices

Parameter	**Instrument**	**Range of measurement**	**Precision**
Solar irradiation	Solar power meter TM-206	0 - 2000 W/m^2	± 5 W/m^2
Temperature in tank	TNA 110, Thermometer type K(CA)	-65 to 1000 ^oC	$\pm$ 1 ^oC
Surrounding wind speed	Anemometer	0 – 20 m/s	± 0.3 m/s

3.3 Performance Analysis

Analysis of the performance of water-in-glass solar water heater involved exposing the evacuated tubes to solar radiations and measuring the initial temperature of water in the storage tank and the final temperature of water in the tank. Heat gained by the system was obtained from Equation (3.1).

$$\dot{Q} = mc_{pw}(T_{out} - T_{in}) \tag{3.1}$$

where Q is is the daily heat gain (MJ), m is the mass of water in the tank (kg), C_{pw} is specific heat of water at constant pressure $(kJ/(kg^oC))$, T_{in} is the initial

temperature of water in the tank (^oC) and T_{out} temperature of water at the tank outlet (^oC).

The efficiency of the system was determined by dividing the power output (heat gained) by the power input. For solar water heaters, the source of energy in the system is solar energy. Solar irradiation, G, received and absorbed by the collector tubes was the power input. This energy was then transferred to the water in the tubes. A natural circulation heat transfer mechanism occurred which heated the water in the storage tank. The efficiency of the system which is generally referred to as instantaneous efficiency was calculated using Equation (3.2) (Tiwari et al., 2018):

$$\eta = \frac{mc_{pw}(T_{out} - T_{in})}{GA_c} \tag{3.2}$$

where η is the efficiency of solar water heater, A_c is the surface area of collector (m^2), G is the solar irradiation (MJ/m^2).

The equation can be written in terms of density and the ratio of solar water tank volume to collector area (Zhang et al., 2014), as

$$\eta = \frac{\rho_w R_{VA} C_{pw}(T_{out} - T_{in})}{G} \tag{3.3}$$

where R_{VA} is the ratio of the storage tank volume to the area of the collector in L/m^2 and ρ_w is the density of water (kg/m^3).

3.4 Uncertainty Analysis

Error in uncertainty analysis is defined as the difference between a true value and a measured value of a physical quantity. The measure of the degree of closeness of an experimental result to a true value is referred to as accuracy while precision is

the degree of how repeated measurements of the same item are close to each other. It is practically impossible to measure a physical quantity without some level of uncertainty. Uncertainty measures the magnitude of the error that have occurred in the measurement of the results (Bevington & Robinson, 2003). Uncertainty analysis which is also known as error analysis is therefore the investigation and estimation of uncertainty in measurements (Taylor, 1997). This analysis helps to determine the accuracy and reliability of the measurements.

Uncertainty in measured values arise from a measuring instrument without perfect accuracy, uncontrolled environmental conditions and the researchers expertise (Ng'ethe, 2015). Experimental and instrumental uncertainties are done to determine the overall uncertainty through repeated measurements of the physical quantity.

3.4.1 Instrumental Uncertainty

Instrumental uncertainty occurs as a result of inaccuracies in the measuring instruments used for the various measurements. The uncertainties in the independent variables help to determine the propagated uncertainty in a dependent variable. The performance analysis of the water in glass evacuated tube solar water heater involved the measurement of solar irradiation, temperature of water inlet, temperature of water outlet and the volume of water in the collector tubes. The volume of water in the tank and the collector area were provided by the system manufacturer while the density of water and the specific heat capacity of water are known with certainty.

The instruments used for measuring these independent variables had some level of uncertainties which propagated into the thermal efficiency of the system. The

overall uncertainty in the efficiency was calculated using Equation (3.4) Equation (3.5) and Equation (3.6) (Bevington & Robinson, 2003).

$$\eta = \eta(T_{in}, T_{out}, G, V) \tag{3.4}$$

$$\frac{\delta\eta}{\eta} = 100\sqrt{\left(\frac{\delta T_{in}}{T_{in}}\right)^2 + \left(\frac{\delta T_{out}}{T_{out}}\right)^2 + \left(\frac{\delta G}{G}\right)^2 + \left(\frac{\delta V}{V}\right)^2} \tag{3.5}$$

- The inlet and outlet temperatures were measured using a TNA 110 thermometer with manufacturers specified precision of $\pm$ 1 ^{o}C ($\delta T_{in,out} = \pm 1$ ^{o}C).
- Irradiance meter with a manufacturers specified precision of ± 5 W/m^2 ($\delta G = \pm 5$ W/m^2) was used to measure solar irradiation.
- A Measuring cylinder with precision of $\pm 3 \times 10^{-6}$ m^3 was used to measure the volume of water in the collector tube.

Equation (3.5) was expressed as

$$U_\eta = 100\sqrt{(U_{T_{in}})^2 + (U_{T_{out}})^2 + (U_G)^2 + (U_V)^2} \tag{3.6}$$

where U_η, $U_{T_{in}}$, $U_{T_{out}}$, U_G and U_V are the uncertainties in efficiency, temperature inlet, temperature outlet, solar irradiation and collector volume measurement. respectively.

From (3.6), the overall uncertainty in the thermal efficiency of the water in glass evacuated tube solar water heater was found to be 3.9%.

3.4.2 Experimental Uncertainty

Experimental uncertainties are classified as random and systematic uncertainties (Taylor, 1997). Random errors are attributed to differences in repeated measurements of the same item while systematic errors result from inaccuracies from poorly calibrated instrument or inaccurate readings by an observer. The measuring instruments were calibrated to eliminate systematic errors from the measurements. Statistical methods are used to analyze random uncertainties in experimental data but not systematic errors. Repetition of the measurements (five different measurements) were carried out to determine the standard deviation of mean (SDOM) which indicates random uncertainty in the results. Determination of the standard deviation of mean involved calculation of the mean and standard deviation of the independent measured values of each variable using Equation (3.7) and Equation (3.8) respectively (Taylor, 1997).

$$\overline{\eta} = \frac{\sum \eta_i}{N} \tag{3.7}$$

$$\sigma_\eta = \sqrt{\frac{1}{N-1}\left(\sum_{i=1}^{n}(\eta_i - \overline{\eta})^2\right)} \tag{3.8}$$

The standard deviation of mean (uncertainty or standard error) was calculated using equation (3.9) (Bevington & Robinson, 2003).

$$\sigma_{\overline{\eta}} = \frac{\sigma_\eta}{\sqrt{N}} \tag{3.9}$$

where $\overline{\eta}$ is the mean of the data, σ_η is the standard deviation, N is the number of data points, $\sigma_{\overline{\eta}}$ is the standard error and η_i is the individual data points. The measured parameters used in the calculation of the thermal efficiency of

the water in glass evacuated tube solar water heater were inlet temperature, outlet temperature, solar irradiation and the volume of water in the collector tubes. Five repeated measurements were taken for each of the parameters for 10 days. The standard deviation and standard deviation of mean (standard error or uncertainty) is presented in Table 3.3. The standard deviation was consistent with the estimate of the instrumental uncertainties and the uncertainty was less than 5.0%.

Table 3.3: Standard Deviation and Standard Error for Parameters

Parameter	**Average value**	**Standard deviation(%)**	**Standard error(%)**
Efficiency	—	3.7	1.6
Solar irradiation	730 W/m^2	3.4	1.5
Inlet temperature	27 ^{o}C	1.9	0.8
Outlet temperature	68 ^{o}C	1.8	0.8
Collector Volume	50 litres	1.2	0.6

3.5 Simulation Model Development and Validation

3.5.1 Design and Sizing of WG-ETSC

The experimental setup of the water in glass evacuated tube solar heater consisted of 20 collector tubes connected directly to a 200 litres horizontally mounted tank. To reduce computational time and resources required, a single-ended tube connected directly to a corresponding portion of the tank was modelled in this study.

The collector tube was inclined at an angle of 23 degrees to the horizontal with a length of 1800 mm and an inner tube diameter of 47 mm. The tank has a diameter of 376 mm, a height of 90 mm and a volume of 10 litres. The thickness of the wall of the inner collector tube was 1.6 mm while the walls of the tank was assumed to be adiabatic with a thickness of 48 mm. These specifications were selected based on the specifications of the experimental setup as shown in Figure 3.3. Figure 3.6 shows the design of the computational model whereas Table 3.4 shows the specifications of the model.

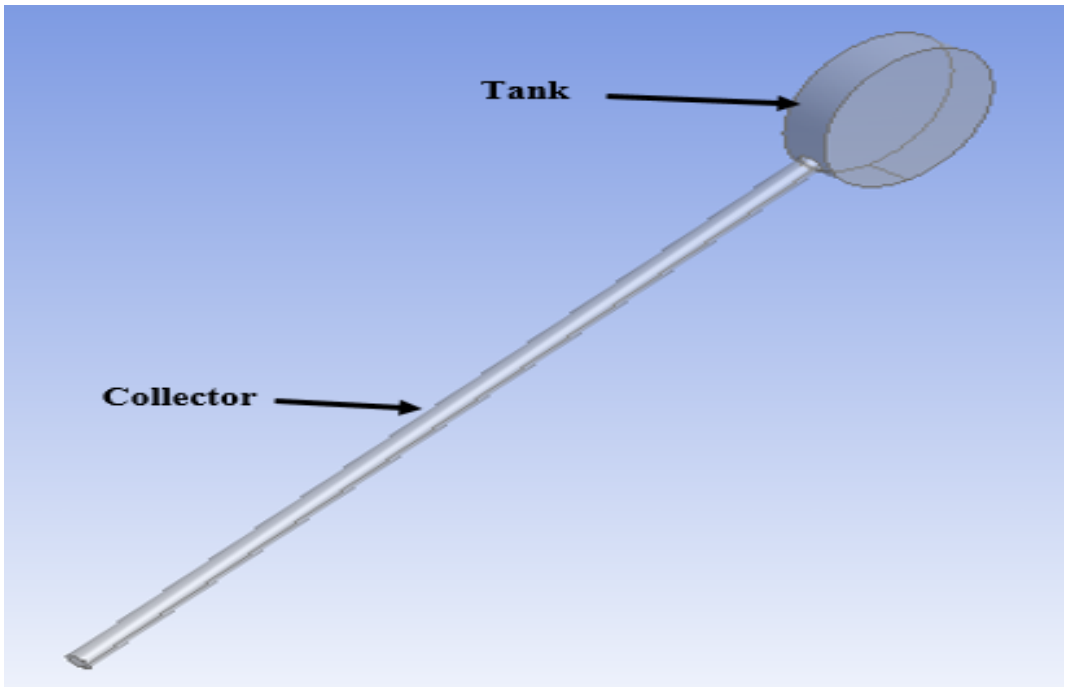

Figure 3.6: Design of Computational Model

Table 3.4: Specifications of Computational Model

S /NO	Element	Specification
1	Tank volume	10 litres
2	Tank diameter	376 mm
3	Tank length	90 mm
4	Collector tube length	1800 mm
5	Collector tube inner diameter	47 mm
6	Collector tilt angle	23 degrees
7	Collector Volume	2.5 litres

3.5.2 Computational Domain of the Simulation

Computational domain and mesh size are critical factors that affect the accuracy of the results obtained from computational fluid dynamics simulation (He et al., 2008). A careful and appropriate selection of the computational domain ensures an accurate prediction of the behaviour of the physical system.

The computational domain for the model consisted of a single collector tube connected directly to a horizontal tank with the axes of the tank and tube perpendicular to each other. The collector tube consisted of the coated inner glass tube responsible for the absorption of solar radiation and the hollow fluid channel for circulation of water. The tank consisted of an inner stainless steel cylinder and an inner space for water circulation and storage.

The plastic painted external casing of the tank, the transparent glass tube, the vacuum space between the two glass tubes of the collector and the header tank

were not included as part of the geometrical model or the computational domain. However, their effect on the performance of the system were incorporated in the boundary condition. The 3-D model was designed using Inventor 2020 and imported into ANSYS design modeller for complete development of the computational domain.

3.5.3 Discretization of the Computational Domain

Grid generation is a key step in numerical simulation because it determines the accuracy and stability of the predictions (Yao et al., 2015). The discretization process involved dividing the computational domain into small units called control volumes along which the governing equations were solved in the simulation process.

ANSYS Meshing Tool was used to discretize the computational domain. To ensure a solution that is independent of the mesh size, stable and accurate, a grid-independent test was conducted taking into account various mesh sizes.

3.5.4 Grid Independence Test

A grid independence test was conducted to ensure a mesh independent solution. Generally, the grid independence test is done to determine the quality and stability of the discretized domain. It ensures a refined mesh size in which a further decrease in the size of the mesh does not affect the solution. A coarse mesh results in inconsistency in the solution and also hinders the solution convergence (Suresh & Regalla, 2014). These limitations can be eliminated through the use of a fine mesh, however, it increases the computational time and space. A medium mesh was used in this study.

Multiple mesh sizes were investigated and their outcomes compared. Five different mesh sizes were tested while holding all other conditions constant. The temperature of water in the tank was observed at particular time intervals.

The initial mesh size was 12 mm with 66829 elements and 13636 nodes. The mesh was then refined to 8 mm, 6 mm, 5 mm and 4 mm respectively. From a mesh size of 6 mm, it was observed that further refinement to 5 mm and 4 mm produced no appreciable change in the results of the simulation as observed in Figure 3.7. Table 3.5 shows the different mesh sizes used in the mesh independence test and their corresponding number of nodes, elements and the output temperatures.

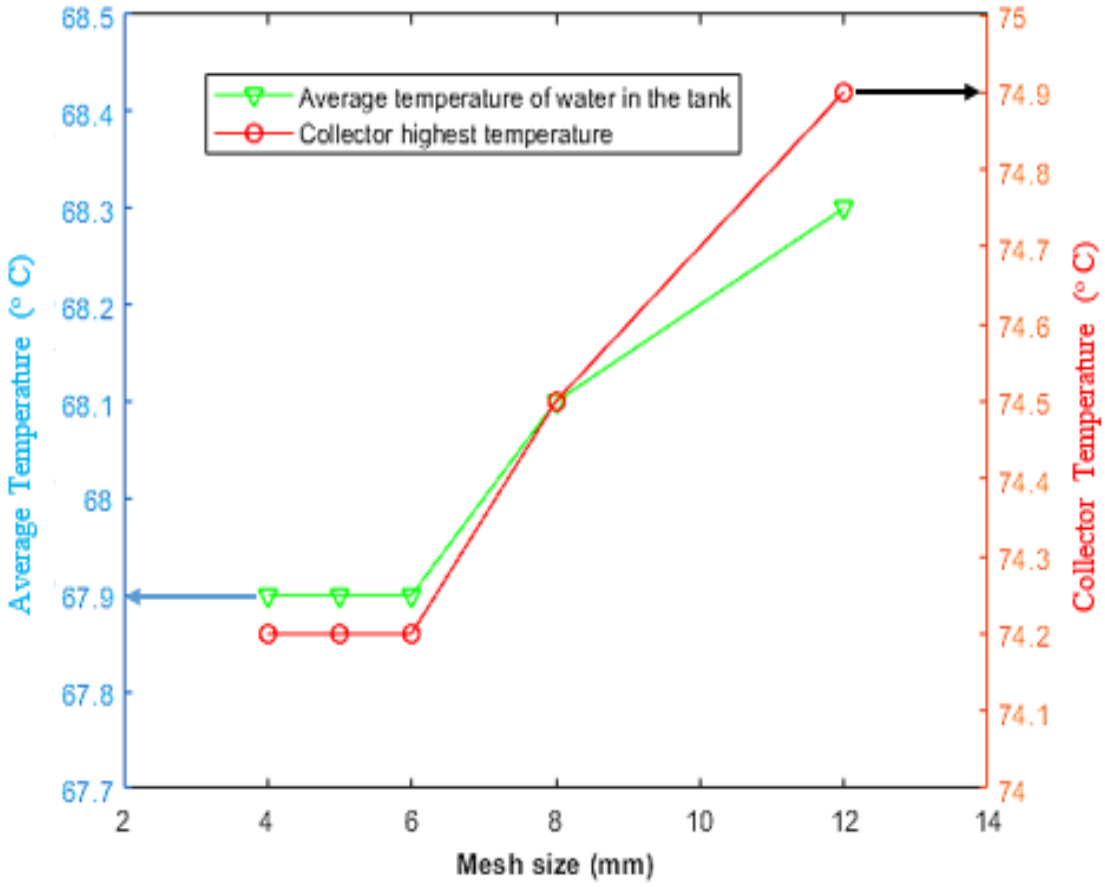

Figure 3.7: Meshed Independence Test

Table 3.5: Mesh Independence Test for the Simulation

Mesh Size [mm]	**Number of Elements**	**Number of Nodes**	**Average Temperature in Tank** $[^oC]$	**Highest Temperature in Collector** $[^oC]$
12	66829	13636	68.3	74.9
8	224811	43121	68.1	74.5
6	526528	97408	67.9	74.2
5	908785	165365	67.9	74.2
4	1776526	318731	67.9	74.2

Based on the data from the grid independence test, a mesh size of 5 mm with 908785 elements and 165365 nodes was used in discretizing the computational domain into control volumes. Figure 3.8 shows the meshed computational domain.

3.5.5 Simulation Assumptions

In CFD simulations, complex physical systems are simplified as much as possible without compromising on the accuracy of the numerical model. The following assumptions were made during the simulation of the WG-ETSWH to simplify its complexity.

1. The intensity of radiation at the upper surface of the tube is uniform.
2. Heat loss from the tank through conduction, convection, and radiation is negligible.

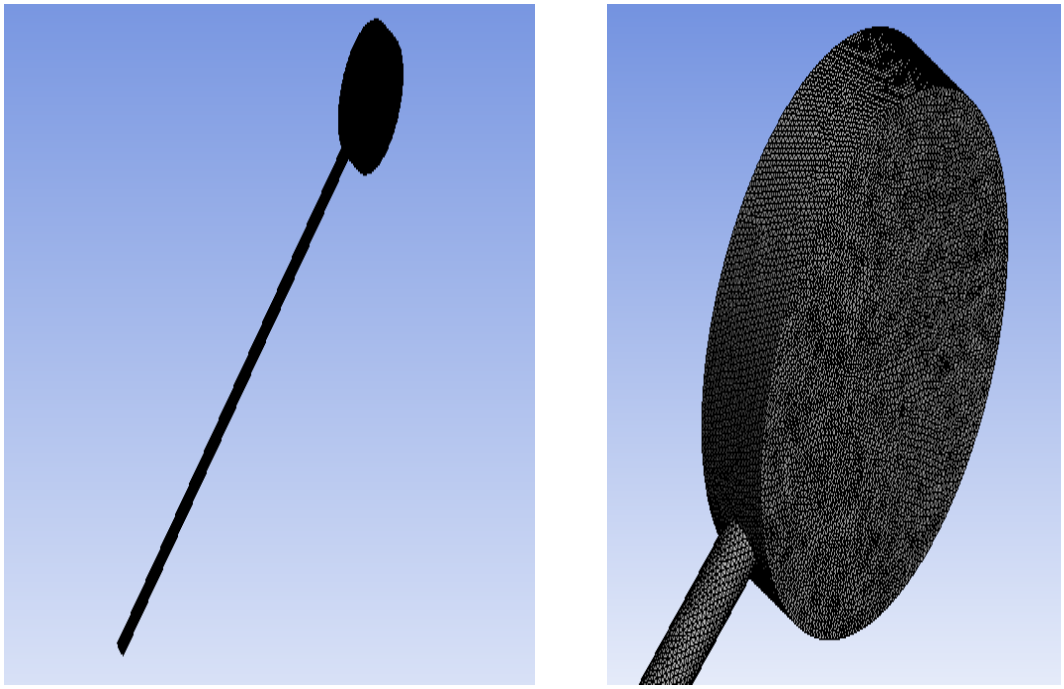

(a) **(b)**

Figure 3.8: Computational Grid for (a) Entire Domain and (b) Portion of Tank

3. No heat transfer between the collector and the surrounding due to the vacuum space between the glass tubes.

4. The tank and the collector are full of water and no air.

5. The flow is internal and incompressible.

6. The flow is laminar and transient.

3.5.6 Flow Governing Equations of Water in Glass ETSC

In this analysis, the system is assumed to be three dimensional, transient and laminar. The following continuity, momentum, and energy equations governing fluid flow were used and are presented in Eq. (3.10), Eq. (3.11) and Eq.(3.12), respectively (Versteeg & Malalasekera, 2007).

Continuity Equation

$$\frac{\partial \rho}{\partial t} + \frac{\partial (\rho u_i)}{\partial x_i} = 0 \tag{3.10}$$

Momentum Equation

$$\frac{\partial (\rho u_i)}{\partial t} + \frac{\partial (\rho u_i u_j)}{\partial x_j} = \frac{\partial}{\partial x_j}(\mu \frac{\partial u_i}{\partial x_j}) - \frac{\partial p}{\partial x_i} + \rho g_i \tag{3.11}$$

Energy Equation

$$\frac{\partial (\rho T)}{\partial t} + \frac{\partial}{\partial x_i}(\rho u_i C_p T - k \frac{\partial T}{\partial x_i}) = 0 \tag{3.12}$$

where

ρ is density, μ is dynamic viscosity, p is pressure, k is thermal conductivity, T is temperature, x_i is position tensor, c_p is specific heat capacity, u is velocity and t is time.

3.5.7 Materials of Computational Domain

The computational domain consisted of the tank and the collector tube. The walls of the tank are opaque and are made of steel while the walls of the collector tube are made of glass. The cell zone contains water in the liquid state. Table 3.6 shows the materials used and their properties.

3.5.8 Boundary and Initial Conditions

Boundary conditions in CFD simulations represent the initial boundary properties and environmental conditions present in the analysis of the physical system. Correct specification of the boundary conditions in numerical simulation represents its approximation of the physical system and also ensures the accuracy of

Table 3.6: Material Properties for Computational Domain

No.	**Materials**	**Density [Kg/m^3]**	**Specific heat [J/Kg.K] at 25 ^{o}C**	**Conductivity [w/m.K] at 25 ^{o}C**
1	Stainless Steel (Engineering Toolbox, 2007)	7840	480	12.7
2	Borosilicate glass (Division Goodfellow Ceramics and Glass, 2008)	2230	750	1.14
3	Water (Fluent, 2018)	incompressible ideal gas	4182	0.6

the simulated result.

The simulation model consisted of the collector tube and the tank. Transient condition was used for this simulation. The Solar ray-tracing model which is built-in ANSYS software was used as the source of solar irradiation. Atmospheric conditions including the day of the year, time of the day, time zone, latitude and longitude of the area were specified together with the sunshine factor.

The collector wall was set as a transparent glass tube which affects solar ray tracing. The walls of the tank were set as opaque and did not affect the ray tracing. The working fluid was water and the initial temperature of water in the system was set as 27 ^{o} C. The flow was assumed to be laminar. The system was assumed to be full of water and no inlet and outlet conditions were assumed. Circulation of water in the system was as a result of the difference in water density at various portions due to uneven heating of water.

Environmental conditions such as atmospheric pressure and temperature were also taken into consideration under the boundary conditions. The boundary conditions used in this simulation are summarized in Table 3.7. These values were selected based on the conditions that existed in the experimental setup.

Table 3.7: Summary of Boundary Conditions

No	Boundary type	Condition
1	Inlet temperature	27 degrees Celsius
2	Collector wall thickness	1.6 mm
3	Tank wall thickness	48 mm
4	Collector tilt angle	23 degrees
5	Sunshine factor	0.7
6	Collector absorptivity	0.96
7	Collector transmissivity	0.04
8	Solar tracing latitude and longitude	-1.03326 and 37.06933
9	Zones of computational domain	Tank, collector, liquid water

3.5.9 Solution Method and Spatial Discretization Schemes

Fluid flow is classified as compressible and incompressible. In incompressible flow, a force applied does not change the density of the fluid to a considerable degree (normally the mach number is less than o.3) and hence its variables can be found using the equation of state. For compressible flows, the volume of the fluid particle can change hence an explicit equation for pressure cannot be determined.

The two solvers used in ANSYS simulations are the pressure-based and density-

based solvers. However, pressure-based solvers are suitable for incompressible and mild compressible flows while density based solvers are suitable for flows which are compressible (Fluent, 2018).

The computational domain was divided into small cells called control volumes. Each control volume has a centre called the nodal point where the properties are defined (Versteeg & Malalasekera, 2007). Discretized equations are then obtained at the nodal point by integrating the governing equation over the control volume. These discretized equations are solved to determine the properties at the node. However, to determine the variables at the faces of the control volume, interpolation methods called spatial discretization schemes are used. The continuity, momentum and energy equations are solved iteratively to obtain velocity, temperature, pressure density, forces and other variables.

The coupled algorithm which is suitable for transient conditions with large time steps was used to deal with the pressure velocity coupling. The spatial discretization schemes used for this study include least squares cell-based for gradient, second-order upwind for both momentum and energy and body weighted force for pressure. Body weighted force is suitable for natural convection flows since it takes into account the discontinuity in the pressure gradient caused by rapid change in density (Fluent, 2018).

3.5.10 Simulation Convergence

Convergence in a CFD simulation is said to be achieved if the change in the solution variables of interest are negligible from one iteration to the other. One way to determine simulation convergence is to monitor the solution residual values. Residuals measure the error between successive solutions of a particular equation

or variable. The lower the residual value, the more accurate the solution.

A Core i3 computer with 4 GB RAM was used for this simulation. A time step of 1 sec was set for the simulation process and it took around 15 hours for completion of a single simulation. The residual value for the momentum equation was less than 0.00001, that of the continuity equation was less than 0.001 while the residual for the energy equation was less than 10^{-11}. Figure 3.9 shows the plot of the residuals from the simulation.

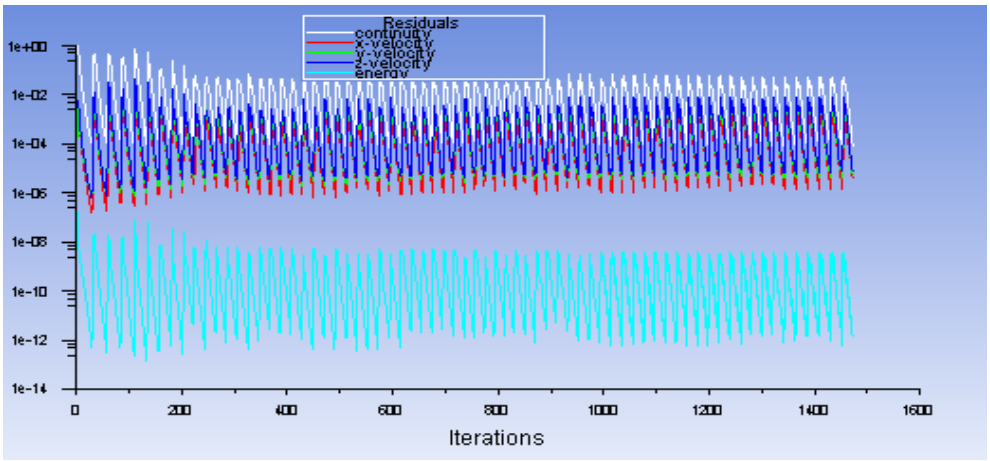

Figure 3.9: Residuals from Simulation

3.5.11 Simulation Processes

ANSYS Fluent package was used for this simulation work. The basis for choosing ANSYS Fluent package is due to its robustness in simulating solar water heating systems and its ability to solve the flow governing equations along with the environmental conditions (Ali Omer Ali, 2019).

A typical simulation process in ANSYS Fluent involves three stages namely pre-processing, solving and post-processing. The following steps were followed in the

simulation process.

- The 3-D computational model was developed using Inventor 2020 software and imported as external geometry into the ANSYS Design Modeller.
- Meshing was then performed in ANSYS Meshing tool by sub-dividing the computational domain into control volumes where the governing equations are to be solved.
- In the setup phase, pressure-based solver which is recommended for incompressible flows was selected. The flow was assumed to be transient since it is time-dependent. Energy as well as solar ray tracing models were activated. Laminar fluid flow was also imposed on the software since the fluid flow in the system is laminar.
- The material properties of the computational domain was defined according to the experimental setup.
- Boundary conditions for the collector tube and the tank were imposed on the software.
- Appropriate solution methods and spatial discretization schemes were selected to calculate the solution parameters from the governing equations.
- Standard and hybrid initialization are the two commonly used methods for initialization of the solution in ANSYS Fluent. Standard initialization was adopted for this study. Time step size, number of time step and number of iterations per time step were specified to calculate the solution until convergence was achieved.

- The ANSYS post-processor was used to display the results of the simulation in form of temperature and velocity contours.

Figure 3.10 shows the flow chart of the simulation process.

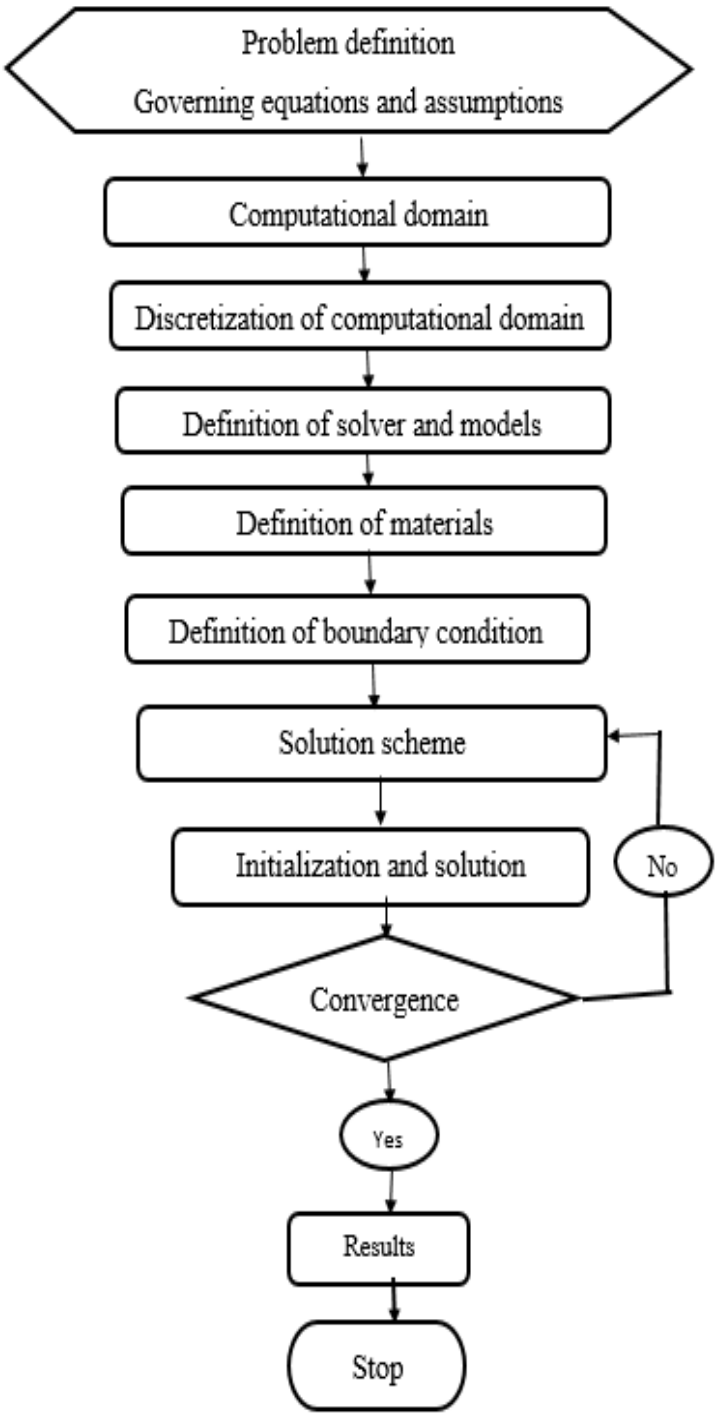

Figure 3.10: Flow Chart of the Simulation Process

3.6 Validation of the Model

The results from the CFD model were compared with experimental data to determine the reliability, accuracy and validity of the CFD model. As mentioned earlier in chapter 3, the CFD model was developed using the specifications of the experimental setup. Additionally, the initial and boundary conditions used in the CFD simulation were selected based on the operating and environmental conditions of the experimental setup. This makes it possible to validate the CFD model using the experimental data.

3.7 Performance Testing Parameters

In the water in glass evacuated tube solar water heater, the collector influences greatly the performance of the system. It is where absorption and conversion of the solar energy from the sun to heat energy takes place. Heat transfer occurs between the inner glass tube and the water circulating within the tube. The rate at which the heat transfer takes place significantly influences the performance of the WG-ETSC.

The sizing of the collector tube and its orientation are critical in the optimization of the thermal performance of water in glass evacuated tube solar water heater. In this research, the length, diameter and tilt angle of the collector tube were explored.

3.7.1 Collector Length Investigation Method

To fully investigate the effect of the collector length on the performance of water in glass evacuated tube solar collector (WG-ETSC), a systematic procedure of varying the length while all other parameters are held constant was adopted. All

other parameters including geometric parameters, initial and boundary conditions, solution methods, discretization schemes were kept constant.

Three different collector lengths were considered for the investigation; collector lengths of 1600 mm, 1800 mm and 2000 mm. Common water in glass evacuated tube solar water heaters available in the market have collector lengths ranging from 1500 mm to 2100 mm. These three collector tube lengths were selected based on the current trend of water in glass evacuated tube solar water heaters existing in the Kenya market. For each of the three collector lengths investigated, a CFD model was developed in ANSYS Fluent.

3.7.2 Collector Tilt Angle Investigation Method

Collector tube tilt angle has a significant effect on the solar energy gain and flow patterns inside the storage tank (Bracamonte et al., 2015). Therefore, to increase the performance of WG-ETSC, an investigation on the effect of the tilt angle of the collector tube needs to be considered. Depending on the geographic location, an optimum tilt angle must be established for optimum performance of the system.

Investigation of the effect of tilt angle on the performance of the system was done using tilt angles of 10, 17, 23, 30, 35 and 45 degrees. These angles were selected within the range of installation tilt angles of water in glass evacuated tube solar water heaters in Kenya. While varying the tilt angle, all other parameters and conditions were held constant.

3.7.3 Effect of Collector Tube Diameter

The exposed surface area of the collector tube affects the rate of solar energy absorption. The surface area of the collector is dependent on its diameter. Additionally, the diameter of the collector tube may also affect the flow patterns in the tube. A need therefore arises to investigate the effect of the tube diameter on the performance of water in glass evacuated tube solar water heater.

To investigate the effect of collector tube diameter, the diameter of the CFD model was varied while keeping all other factors constant. The diameters used for the investigation were 42 mm, 47 mm and 52 mm. These diameters take into account the minimum, maximum and average diameters of water in glass evacuated tube solar water heaters in the Kenya market.

3.8 Optimization of the Thermal Performance of WG-ETSWH

Optimization is defined as the process of obtaining conditions that give a maximum or minimum value of a function (Rao, 2009). It involves finding the best results for a particular problem or circumstance. The ultimate aim of the optimization process is either to minimize the effort required or maximize the desired benefit (Menon, 2005). ANSYS design exploration was implored to optimize the performance of the WG-ETSWH.

The optimization process in ANSYS involves an initial design of the CFD model, meshing of the computational domain, setup and solution and post-processing of the results. The input and output parameters are specified during the simulation process. These input and output parameters are the critical variables that needs

to be maximized or minimized in the optimization process. The input and output parameters are classified as design variables, state variables and objective variable in ANSYS (Beňo et al., 2014). Design variables are the independent parameters that directly affect the output of the system while state variables depend on the design variables and changes accordingly with a change in the design variables.

Collector tube length, collector tilt angle and collector tube diameter were set as input parameters. Output parameters for the optimization process were the average temperature in the storage tank, average system velocity and solar heat flux on the collector surface. These were used as objective variables in the optimization process. Response surface optimization model was selected for the design exploration analysis. Response surface optimization involves the design of experiment, surface response and finally optimization.

3.8.1 Steps in Response Surface Optimization

1. Design of experiment
2. Surface Response
3. Optimization

3.8.2 Design of Experiments

Design of Experiments is defined as the process of planning, designing and analyzing experiments to effectively draw a valid and objective conclusion (Antony, 2014). Design of experiments in ANSYS involves defining the input parameters (design variables) and the output variables. Design variables specified were collector length, collector diameter and collector tilt angle. The lower bound and the upper bond for each design variable was specified as shown in Table 3.8

Table 3.8: Lower and Upper Bound for Various Design Variables

No	Design variable	Lower bound	Upper bound
1	Collector length	1500	2100
2	Collector diameter	42	52
3	Collector tilt angle	10	45

Output parameters specified for the design of experiments include average temperature in the storage tank, average velocity and solar heat flux. The optimal space filling was selected as an experiment type and max-min distance as design type. Optimal space filling method spreads the design points uniformly within the design space. Max-min distance ensures that no two data points are very close to each other (Fluent, 2018).

3.8.3 Surface Response

Response surface describes the output parameters in terms of the input parameters (Fluent, 2018). Response surface data are obtained from the design of experiment data. It generates approximated values for the output parameters from the design of experiments.

The non-parametric regression method was set as the response surface type. It predicts output parameters by using an important data point as a reference and the response produced is of a high quality.

3.8.4 Optimization

The optimization process of the water in glass evacuated tube solar water heater was conducted using the Multi-Objective Genetic Algorithm (MOGA) method. The MOGA method can operate with all kinds of input parameters and can also handle multiple objectives (Fluent, 2018). The number of initial samples used is 500 and the number of samples per iteration was set to 200. A larger initial sample size enhances the chance of obtaining the input parameters with the best output.

The domain for the collector length ranges from 1500 mm and to 2100 mm, the domain for the collector tilt angle was from 10 to 50 degrees and that of the collector diameter was from 42 mm to 54 mm. The objectives and the constraints set for the output parameters are represented in Table 3.9. The solution of the

Table 3.9: Optimization Objectives and Constraints

Parameter	**Objective**	**Constraint**
Average water temperature in tank	Maximize	Values greater than Lower bound
Average flow velocity	Maximize	Values greater than lower bound
Solar heat flux	Maximize	No constraint

optimization problem converged after 1386 evaluations.

CHAPTER FOUR

RESULTS AND DISCUSSION

4.1 Overview

This chapter presents the thermal performance of water in glass evacuated tube solar water heater under the climatic conditions in Kenya, investigated both experimentally and numerically. The findings on effect of collector tube length, collector diameter and collector tilt angle on the performance of the system is also presented and discussed in this chapter.

4.2 Performance of Water in Glass Evacuated Tube Solar Water Heater

4.2.1 Atmospheric Conditions

The solar irradiation at the study area increased in the morning until 1:00 pm where a maximum irradiation was recorded and then a gradual reduction in the irradiation was observed until 6 pm. An increasing trend in ambient temperature was observed from the morning hours until around 2 pm where the ambient temperature begins to decrease.

The maximum ambient temperature recorded during the study period was 33 ^{o}C. The study was conducted during the months of January and February, 2021.

Figure 4.1 shows a typical irradiation and atmospheric temperature recorded on the 28th of January, 2021.

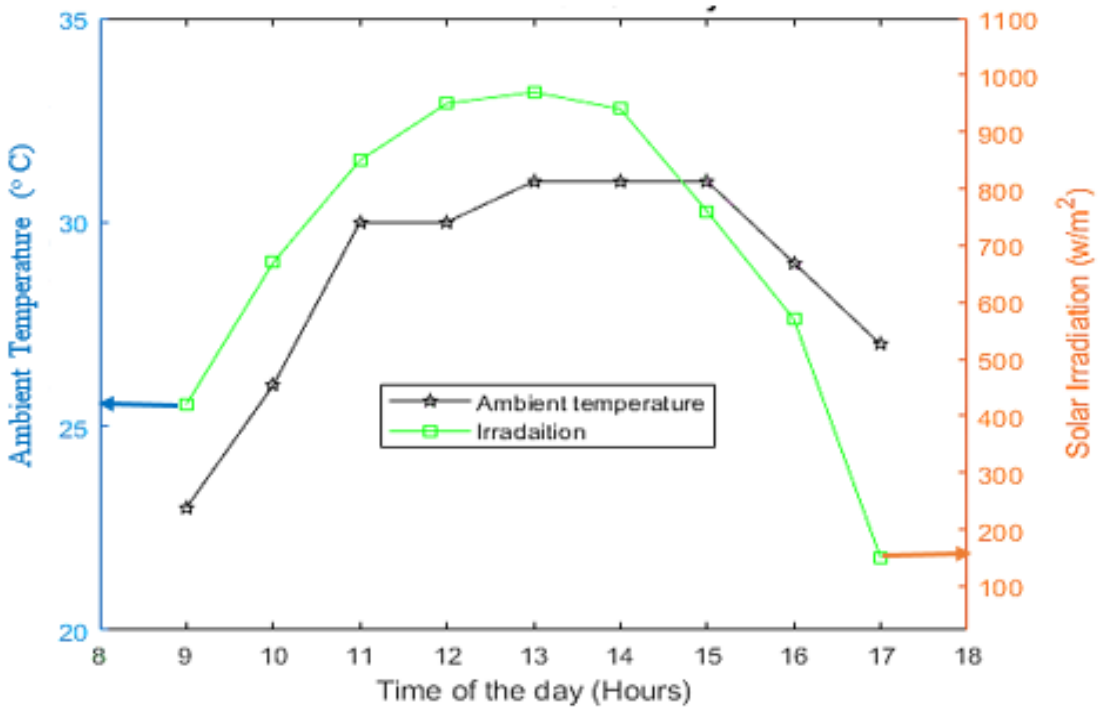

Figure 4.1: Ambient Temperature and Irradiation on 28th January

4.2.2 Temperature Distribution in the Tank

Daily measurement of the temperatures in the tank were taken from 9:00 am to 5:00 pm. Temperatures at the top portion, middle portion and bottom of the tank were measured at points within the tank as shown in Figure 3.5. Figure 4.2 shows the temperature distribution of water at the bottom, middle and top portions of the tank at various hours of the day for two different days. T_u is the temperature of water at the top of the tank, T_m is the temperature at the middle of the tank and T_b is the temperature at the bottom of the tank as seen in Figure 3.5.

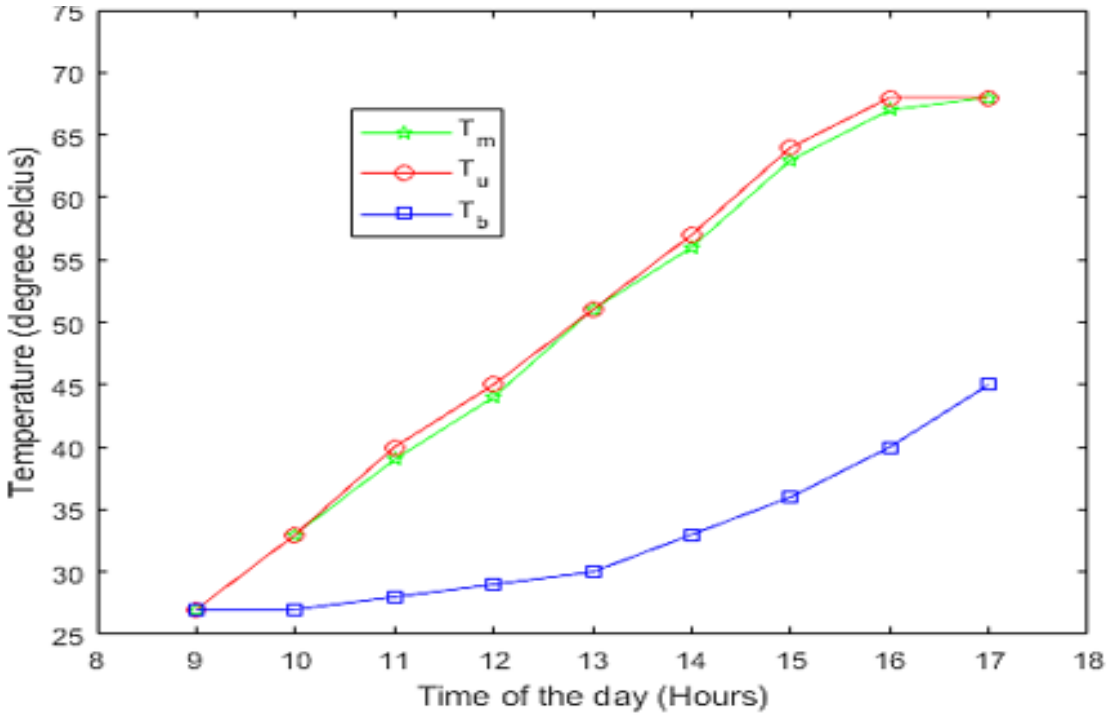

(a) 28th January, 2021,

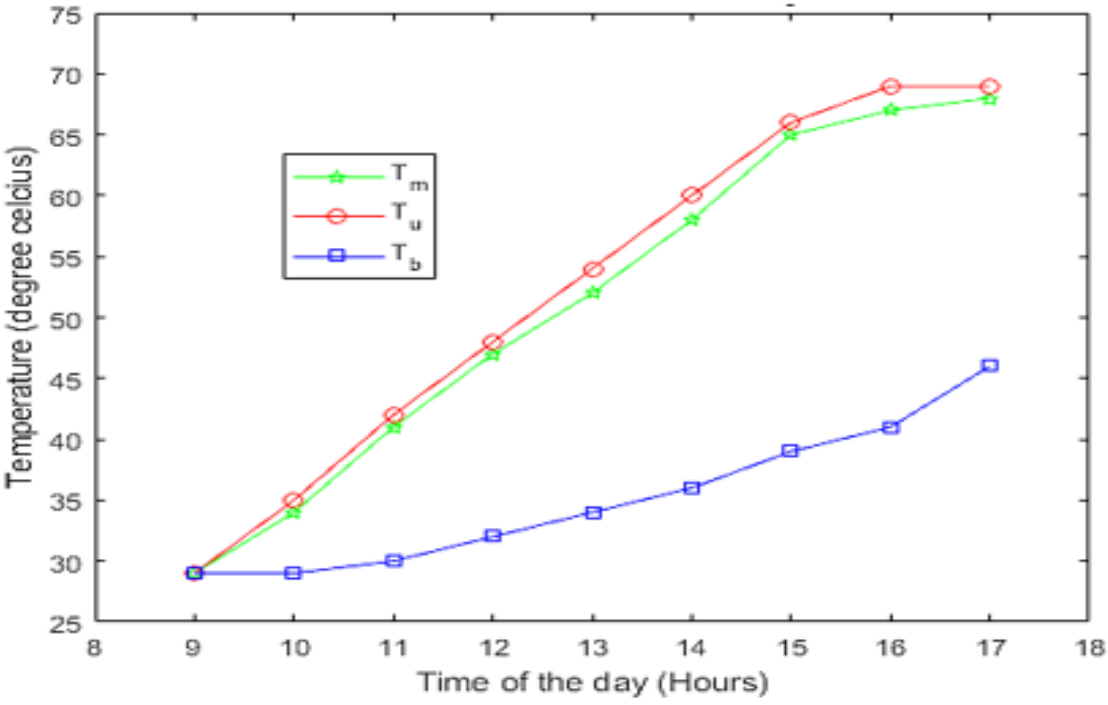

(b) 29th January, 2021

Figure 4.2: Temperature Distribution at Various Points in the Tank

Temperature variations were observed at different points in the tank. The deviation in water temperature at the middle portion and the top portion of the tank is negligible. However, a major deviation in water temperature is seen between the middle portion of the tank and the bottom of the tank. A temperature difference of about 23 ^{o}C was observed between the water at the bottom of the tank and the water at the middle portion of the tank on 28th January, 2021 at 5:00 pm. Similar results were recorded for the other days in the study period.

This is attributed to the fluid transfer between the evacuated tubes and the tank (Morrison et al., 2004). The evacuated tubes are inclined at an angle to the tank and hence leaves a portion of the water in the tank below the tubes thermally inactive. Since the hot water returning from the tubes is less dense compared to the cold water below the tubes in the tank, penetration of hot water to the bottom of the tank through natural circulation is hindered which leads to low water temperature at the bottom of the tank. This reduces the fraction of hot water in the tank available for use at any point in time. These results agree with the work done by Morrison et al. (2004), Tang et al. (2011) and Bracamonte et al. (2015), who predicted the presence of a thermally inactive region at the bottom of the storage tank. The fraction of hot water within the tank can be increased sufficiently by increasing the tilt angle of the tubes and reducing the length of the tubes inside the tank.

4.2.3 Rate of Cooling in the Night

The hot water in the tank is retained throughout the night until the next morning. The temperature of water at the top, middle and bottom portion of the tank were recorded at 7:00 am to determine the rate of cooling in the tank during the night.

A uniform water temperature was recorded at the middle and at the upper portions of the tank for the various days while the temperature of water at the bottom (below tube opening) remained lower than at the portions above the opening of the tube. Table 4.1 shows the temperature distribution in the tank at 9:00 am, 5:00 pm in the evening and 7:00 am of the following day.

Table 4.1: Temperature Distribution in the Tank During the Evening and in the Morning of the Following Day

Date	**Initial temperatures (9:00 am)**		**Evening (5:00 pm)**		**Morning of following day (7:00 am)**	
	Tm(^{o}C)	**Tb(^{o}C)**	**Tm(^{o}C)**	**Tb(^{o}C)**	**Tm(^{o}C)**	**Tb (^{o}C)**
26th January, 2021	28	28	64	42	55	52
28th January, 2021	27	27	68	45	59	55
29th January, 2021	29	29	69	46	60	55

The temperature distribution shows a decrease in temperature of water at the portion above the tube opening in the tank and a rise in temperature of water at the portions below the tube opening in the tank from 5:00 pm to 7:00 am as observed in Table 4.1. At the portions above the tube opening, a decrease

of about 9 ^{o}C in water temperature was recorded for the 14 hour period of no significant solar irradiation whilst a temperature rise of about 10^{O}C was recorded at the bottom of the tank.

Figure 4.3 shows the distribution of water temperature in the tank for 22 hour period as observed on 28th January, 2021.

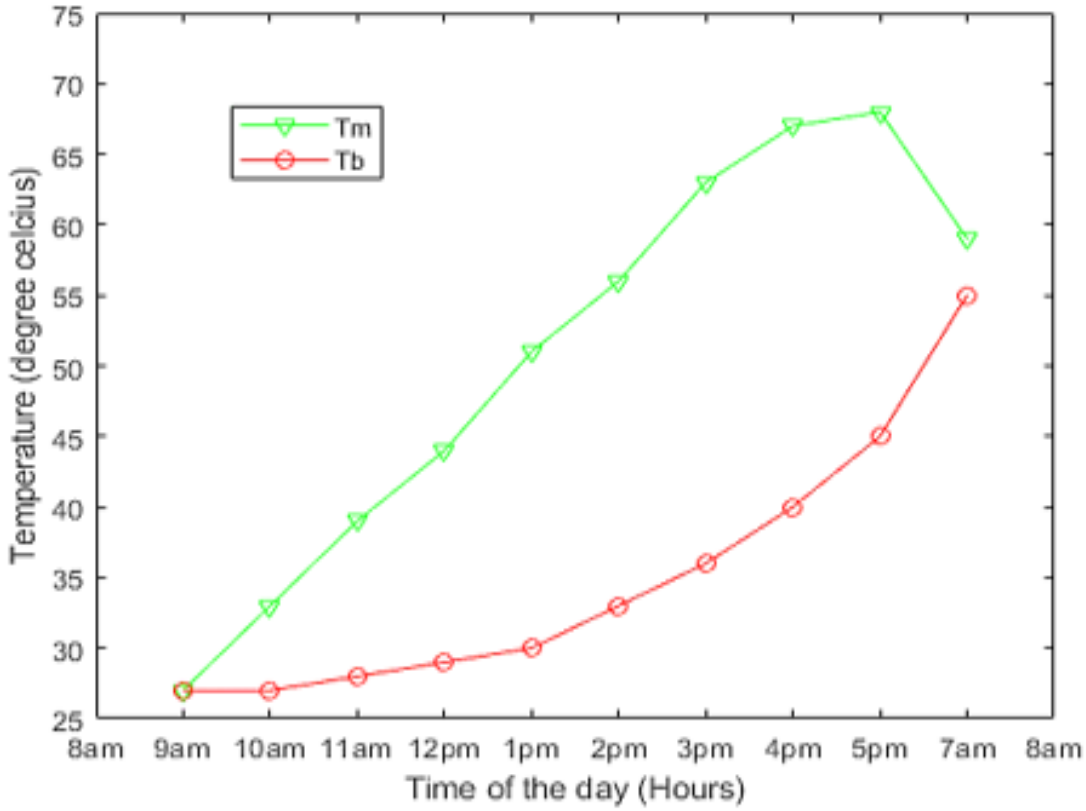

Figure 4.3: Temperature Distribution at the Upper Portion and at the Bottom of the Storage Tank on 28th January, 2021.

This observation was attributed to the natural convection heat transfer that occurs between the hot water at the top of the tank and the cold water at the bottom of the tank. This phenomenon tends to establish a uniform temperature in the tank in the absence of solar radiations in the night. Mixing of the hot water

above the tube opening in the tank with the cold water below the tube opening occurred which led to a decrease of about 9 ^{o}C in the temperature of water at the upper part of the tank. Heat transfer between the solar water heater and the ambient air is minimum during the night.

4.2.4 Performance of Water in Glass Evacuated Tube SWH

The performance of water in glass evacuated tube solar water heater was investigated using 20 tubes connected directly to a 200-litre tank. Each collector tube has a volume of 2.5 litres. The total volume of the 20 collector tubes is 50 litres. The system was filled with water in the morning and allowed to operate until 5 pm without drawing water from it. The initial temperature in the morning was recorded as T_{in} and the final temperature in the evening was measured as T_{out}. Corresponding irradiation levels were measured to determine the efficiency of the system. The efficiency was calculated using Equation (3.3). Figure 4.4 shows the daily solar irradiation and the corresponding daily efficiency of the system.

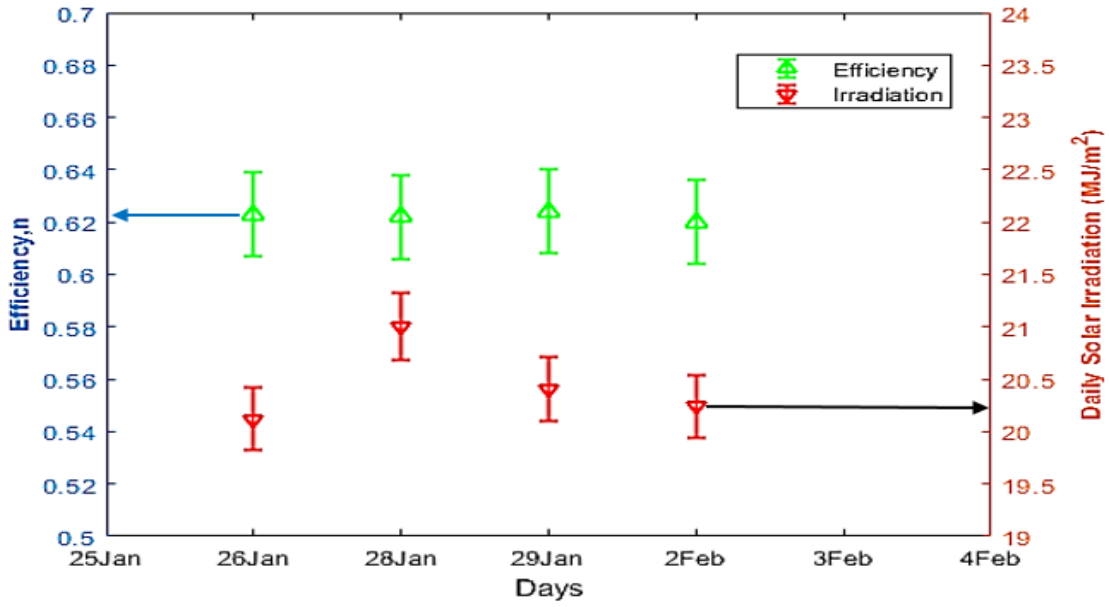

Figure 4.4: Performance of Water in Glass Evacuated Tube SWH

The amount of daily incident irradiation has a great influence on the final temperature of the system. Heat gained by the water in the tank is relatively high for higher solar irradiation. The heat gained by the system was calculated using Equation (3.1). The highest solar irradiation for the study period occurred on 28th January, 2021 with solar irradiation of 21 MJm^{-2} and a corresponding heat gain of 42.85 MJ. Therefore, placing the solar water heater at a point of maximum solar irradiation incidence is beneficial for optimum heat gain.

The efficiency of water in glass evacuated tube solar water heater was found to be in the range of 58% - 65% under the climatic conditions of Juja, Kenya. Atmospheric and climatic conditions have a great impact on the performance of WG-ETSWH. Since the climatic conditions in Kenya vary from one region to another, there is a need to investigate the performance of WG-ETSWH in other parts of the country.

4.3 Simulation Results and Validation

4.3.1 Performance of CFD Model

The CFD model of the water in glass evacuated tube solar water heater was simulated using the methods described above together with the environmental conditions that existed in the experimental set up. From the simulation results, the temperature of water in the collector tube was higher than the temperature of water in the storage tank. The bottom portion of the collector tube was found to have the highest water temperature. The average temperature of water in the storage tank was found to be 67.9 ^{o}C.

Figure 4.5 shows the temperature distribution in the CFD model.

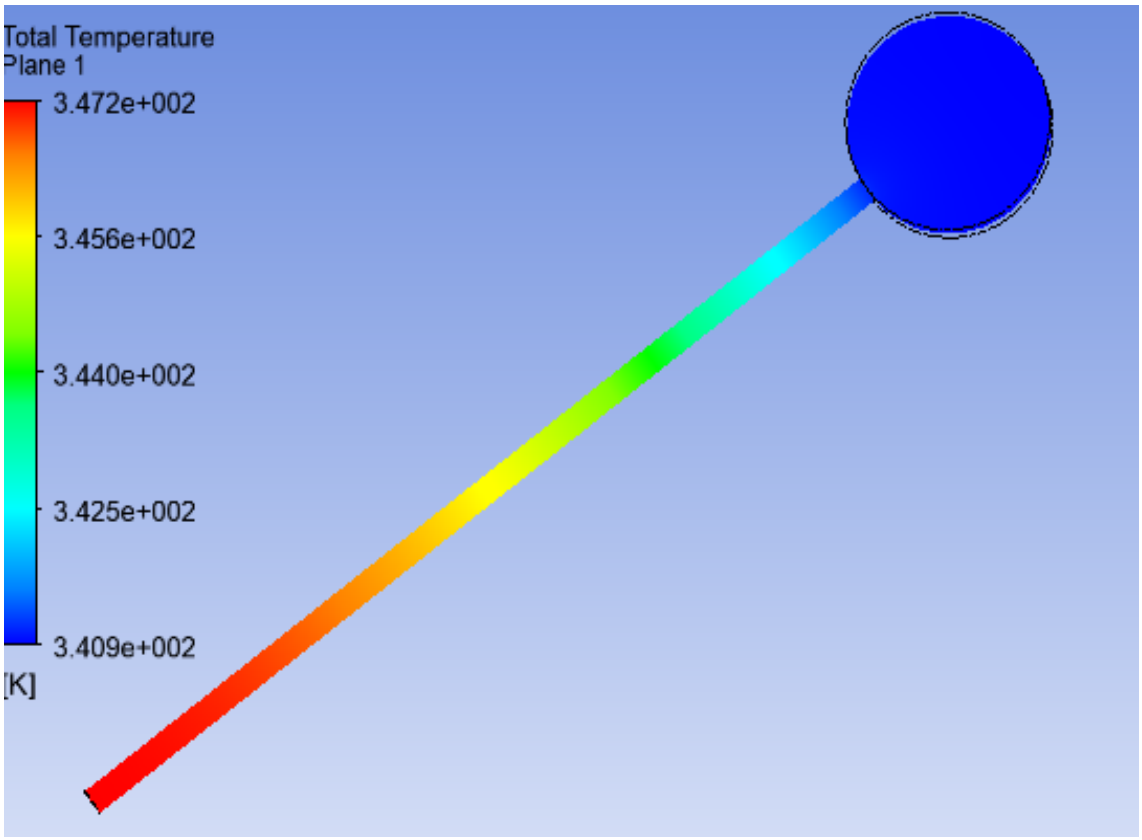

Figure 4.5: Temperature Distribution in the CFD Model

The flow velocity was found to be higher at the upper regions of the collector tube near the storage tank and at the regions around the tube opening in the storage tank. This behavior may be attributed to the high mixing rate of the cold water from the storage tank and the hot water from the collector tube at these regions due to the high temperature difference. However, a region of water stagnation was observed at the bottom of the collector tube. The average flow velocity in the system was 0.000174 ms^{-1}. Figure 4.6 shows the velocity distribution in the CFD model.

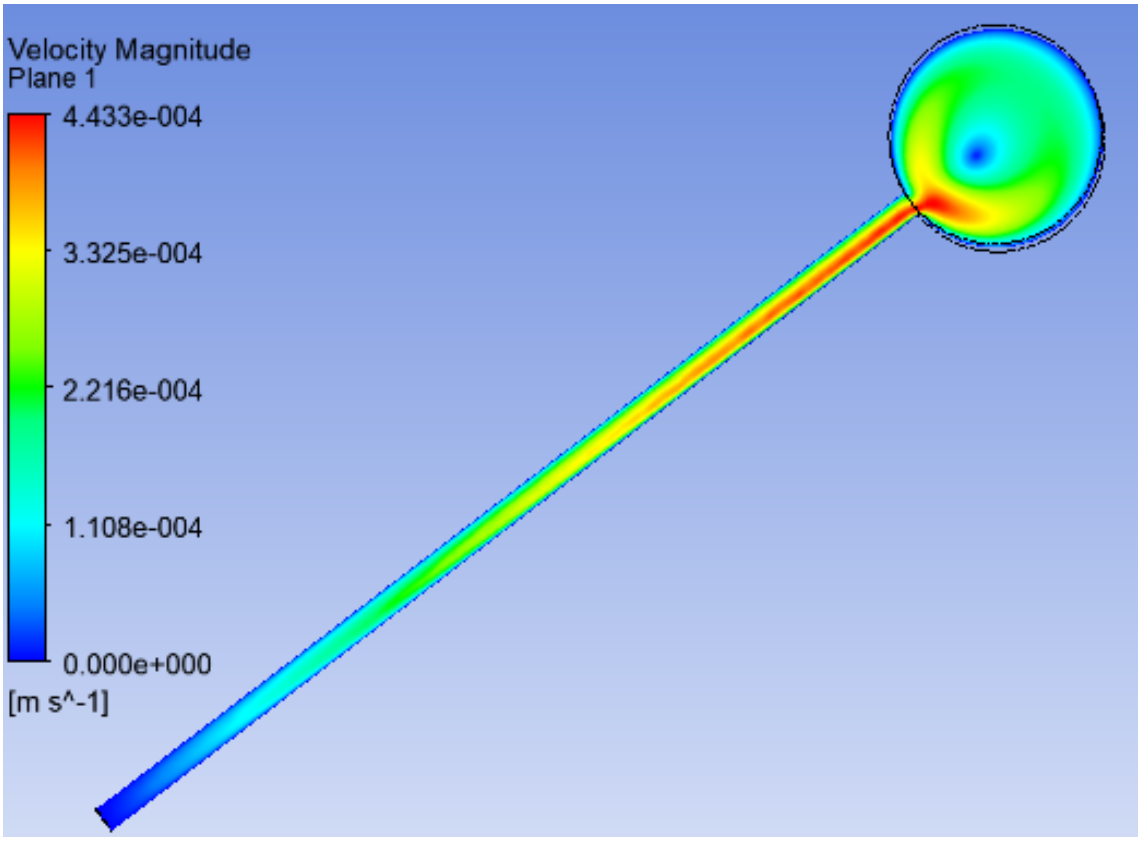

Figure 4.6: Velocity Distribution in the CFD Model

4.3.2 Validation of the Performance of CFD Model

To ensure the validity of the CFD model for further analysis, the results from the simulated model were compared to the results from the experimental setup. Table 4.2 shows a comparison of the experimental results with the simulation results for data obtained on 28th January, 2021. The initial temperature of the water in the system was 27^o C. The data shows an average deviation of 0.23 % of the simulated results from the experimental results.

This close agreement proves the validity and accuracy of the simulation model and hence can be used to represent the real system for further studies.

Table 4.2: Comparison of Experimental and Simulation Results

Time	**Radiation** $[W/m^2]$	**Experimental** T_{out} $[^o C]$	**Simulation** T_{out} $[^o C]$	**%Error**
9 am	420	27	27.0	0
10 am	670	33	31.7	0.42
11 am	850	39	38.1	0.29
12 pm	950	44	44.4	0.17
1 pm	970	51	50.6	0.12
2 pm	940	56	56.5	0.15
3 pm	760	63	62.3	0.20
4 pm	570	67	67.9	0.26

4.4 Effect of Geometric Variables on Performance from Simulation

4.4.1 Effect of Collector Tube Length

Collector tube lengths of 1600 mm, 1800 mm and 2000 mm were used to investigate the effect of the length of the collector tube on the performance of water in glass evacuated tube solar water heater. Results from the simulation revealed that the length of the collector tube affects the heat gain and hence the temperature output of the system. The model with the longest collector tube length (2000 mm) achieved the highest water temperature of about 70.5 ^{o}C whilst the lowest temperature recorded was for the shortest tube length of 1600 mm. The lowest temperature recorded was 337.8 ^{o}C

The temperature distribution in the tank for the various tube lengths are pre-

sented in Figure 4.7.

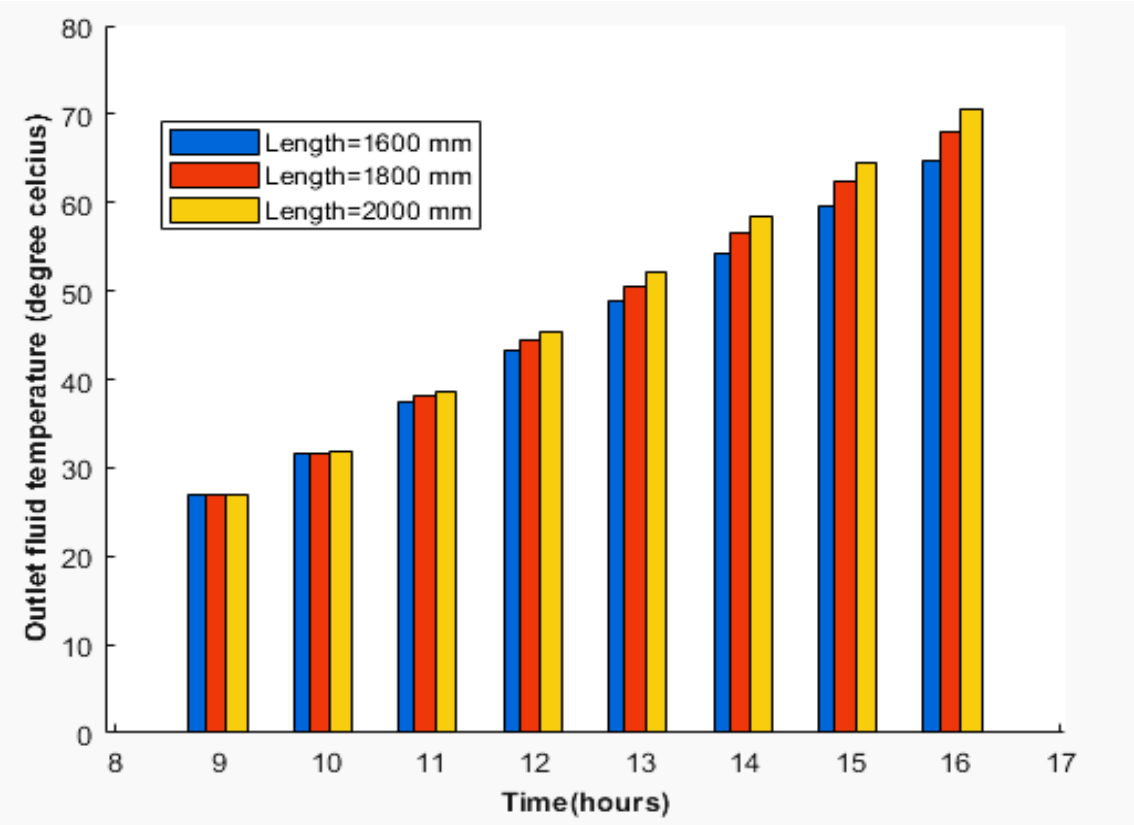

Figure 4.7: Temperature Distribution for Various Tube Lengths

Increasing the length of the collector tube increases the surface area of the collector exposed to the sun for solar absorption. Additionally, it increases the volume of water in the tube available for the heat transfer process between the tube walls and the water inside the tube. This accounts for the increase in temperature as the length of the collector tube increases. This results agree with the work done by Shah & Furbo (2007) on all glass evacuated tubes. However, in the determination of the optimum length of the collector tube, the installation space and ease of transportation of WG-ETSWH must also be taken into consideration.

The hot water at regions close to the sealed end of the collector tube was found

to be stagnant for all three cases. The rate of water circulation between the tank and the collector tube was found to be very high for longer collector tubes as observed in Figure 4.8. The longest collector tube length (2000 mm) attained an average flow velocity of 0.0002 ms^{-1} while the shortest collector tube length (1600 mm) attained an average flow velocity of 0.00015 ms^{-1} . This observation may be attributed to the high heat gain recorded for longer collector tube. This resulted in rapid changes in density enhancing the natural circulation flow rate.

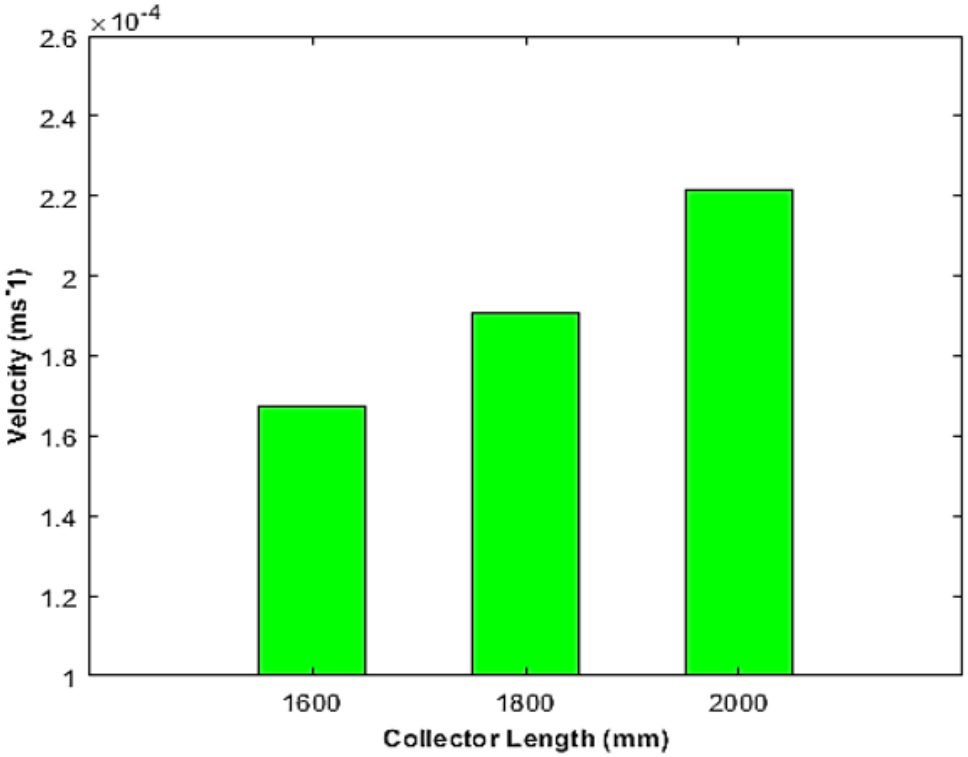

Figure 4.8: Average Velocity for Various Tube Lengths

4.4.2 Effect of Collector Tilt Angle

The effect of the collector tilt angle on the performance of water in glass evacuated tube solar water heater was investigated using tilt angles of 10, 17, 23, 30, 35 and 45 degrees. The collector tube of WG-ETSWH is normally placed at a particular

angle to absorb maximum solar radiation from the sun. The experimental setup was placed at an angle of 23 degrees. A constant tube length of 1800 mm was used while varying the tilt angles. Results from the simulation showed that within the range of the tested tilt angles, the average water temperature in the storage tank increases with an increase in tilt angle until 30 degrees where the average temperature begins to decrease. The highest average water temperature recorded (67.87 ^0C) was for tilt angle of 30 degrees. However, the change in water temperature due to changes in tilt angle was marginal. The temperature distribution of water in the tank for the various tilt angles are shown in Figure 4.9

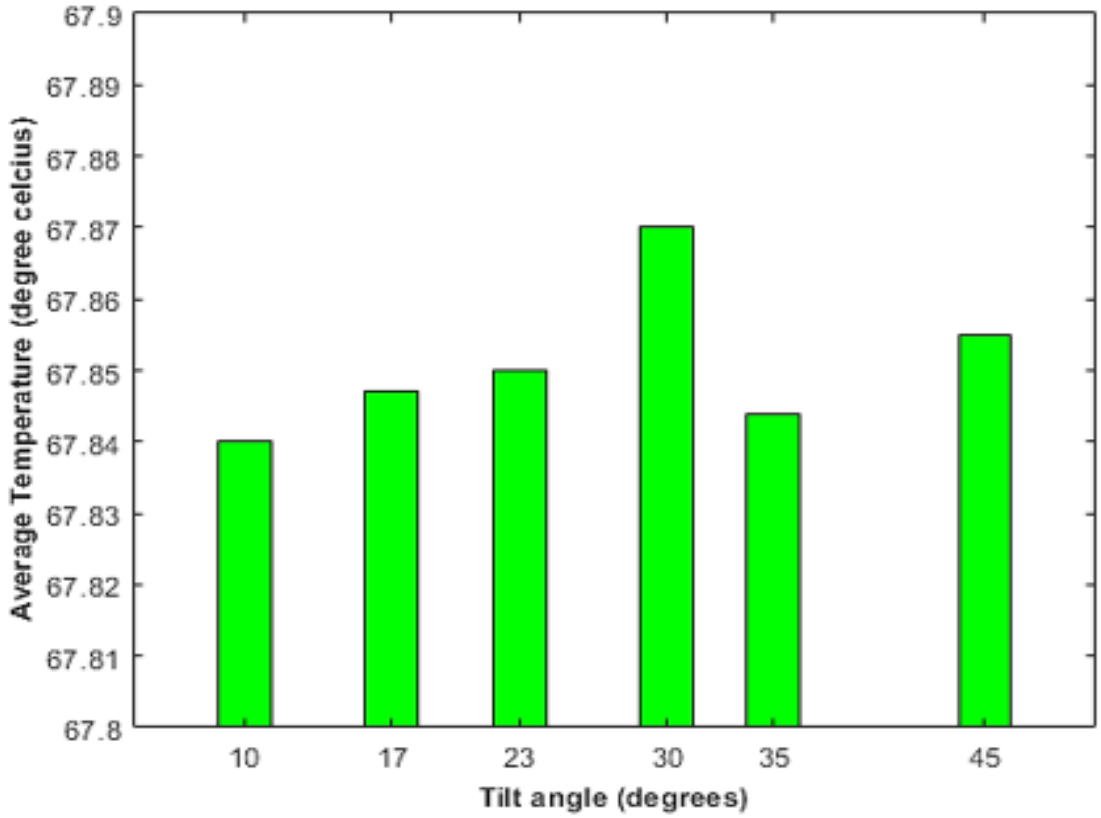

Figure 4.9: Temperature Distribution for Various Tilt Angles

However, a decrease in the average flow velocity was observed when the tilt angle of the collector was increased from 10 degrees to 45 degrees. The highest tilt angle (45 degrees) recorded the lowest average flow velocity as presented in Figure 4.10. The average flow velocity recorded for a tilt angle of 10 degrees was 0.000179 ms^{-1} whereas 0.000159 ms^{-1} was recorded for a tilt angle of 45 degrees. This observation was attributed to the natural circulation which occurred between the tank and the collector tubes. For lower tilt angles, water easily flows from the tubes to the tank as compared to higher tilt angles. Additionally, the possibility of stagnant region at the bottom of the collector tube for higher tilt angles might be a cause for the lower average velocity recorded for higher tilt angles.

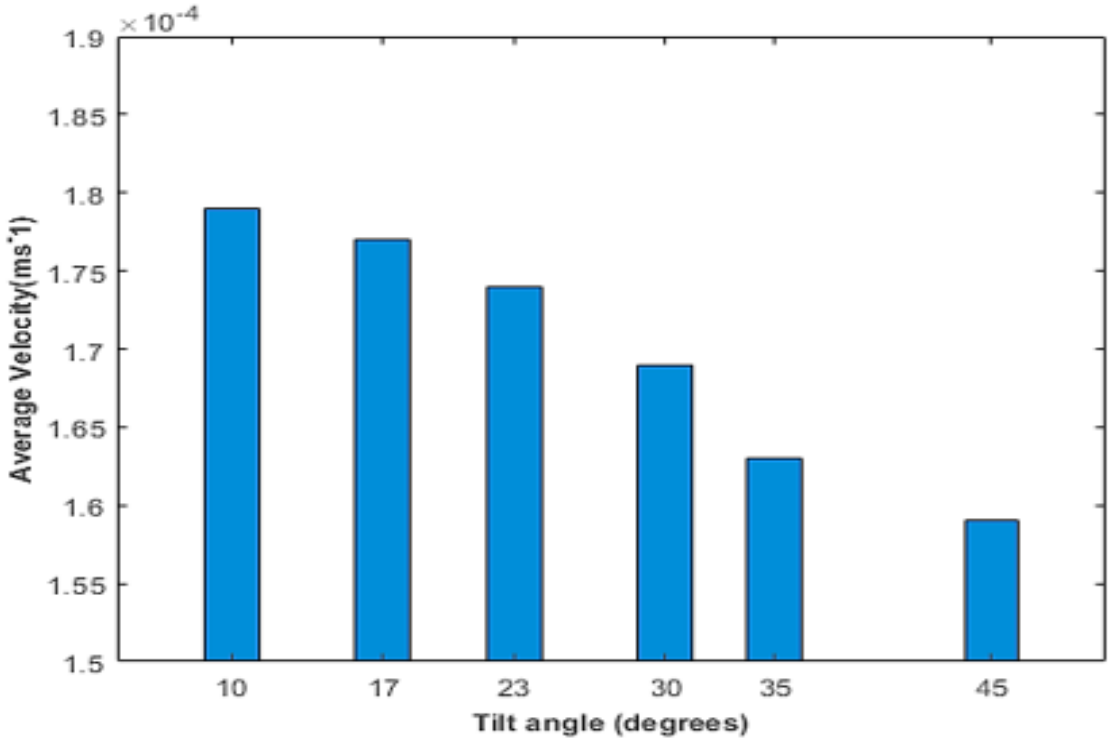

Figure 4.10: Average Velocity for Various Tilt Angles

The maximum flow velocity in the collector tube occurred at regions near the

tank. It was observed that the flow velocities at the upper portions of the collector tube was very high for higher tilt angles. The maximum velocity recorded for tilt angle of 45 degrees was 0.000529 ms^{-1} while the maximum velocity recorded for tilt angle of 23 degrees was 0.000486 ms^{-1}. This increases the kinetic energy at the tube opening for high tilt angles which subsequently enhances the mixing of the hot and cold water in the storage tank. This finding agrees with the work done by Bracamonte et al. (2015). The former author stated that low tilt angles results in stratification of the water content below the tube openings.

The deviation of the average flow velocity from the maximum flow velocity recorded for the various tilt angles may be attributed to a possible greater stagnation region at the bottom of the collector tube for higher tilt angles.

4.4.3 Effect of Collector Tube Diameter

To establish the influence of collector tube diameter on the performance of water in glass evacuated tube solar water heater, three different collector tube diameters were investigated while holding all other parameters constant. The diameters used for the investigation were 42 mm, 47 mm and 52 mm. The diameter of the collector tube of the experimental setup was 47 mm. The diameter of the collector tube determines the exposed surface area of the collector available for absorption of solar irradiation.

Results from the simulation indicated that the diameter of the collector tube has a significant influence on the temperature gain of the water in the storage tank. When the diameter of the collector tube was increased, the temperature of the water in the storage tank rose significantly as shown in Figure 4.11

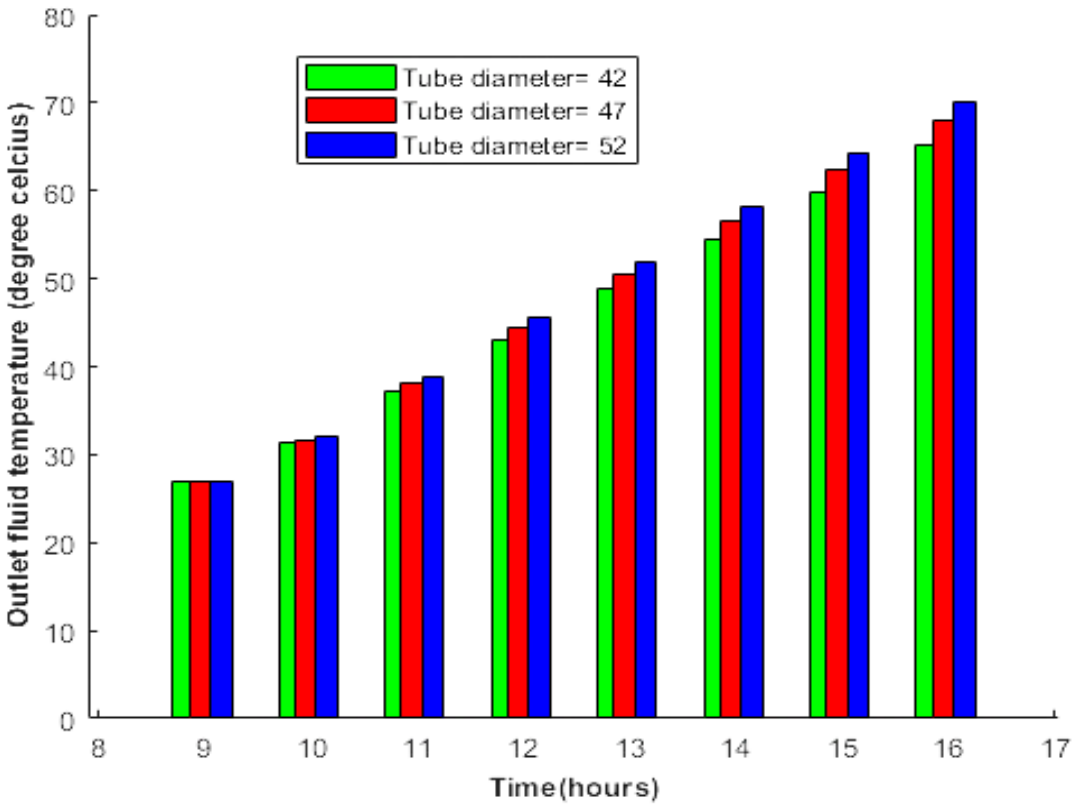

Figure 4.11: Average Temperature in the Tank for Various Diameters

An increase in the diameter of the collector tube resulted in an increased surface area of the collector. This in turn increases the solar irradiation incident on the collector surface. However, several factors such as number of collector tubes, the length of the storage tank and the distance between the centres of adjacent collector tubes must be taken into consideration in the determination of the optimum tube diameter.

Figure 4.12 shows the velocity distribution for the various collector tube diameters. From the distribution, collector tube diameter of 42 mm recorded the highest average velocity of 0.00018 $ms^{-}1$ while collector tube diameter of 52 mm recorded the lowest average velocity of 0.000169. Increasing the collector tube diameter resulted in a decrease in the average flow velocity.

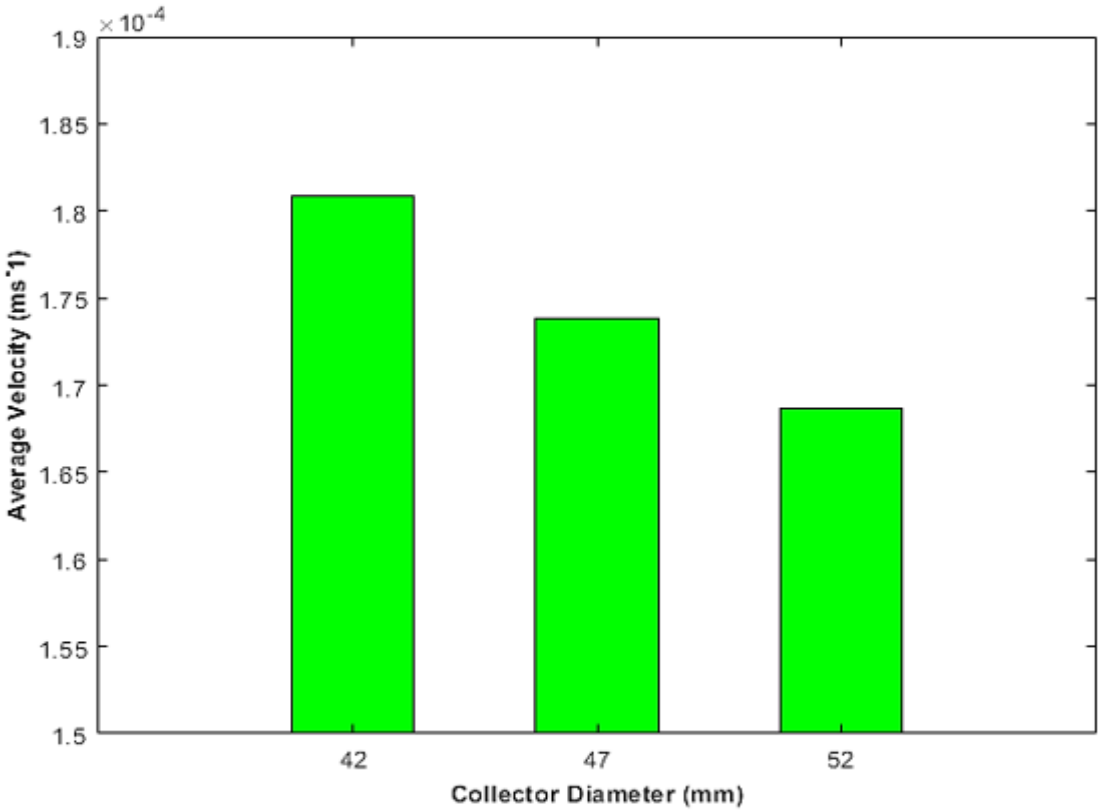

Figure 4.12: Average Velocity for Various Tube Diameters

4.5 Optimization of WG-ETSWH

Optimization of the WG-ETSWH was conducted using three main design variables namely, collector tube length, collector tube diameter and collector tilt angle. Response surface chart which shows the magnitude of impact of each design variable on the output parameters were plotted. The average temperature of the water in the storage tank was found to be highly responsive to the change in collector length as shown in Figure 4.13.

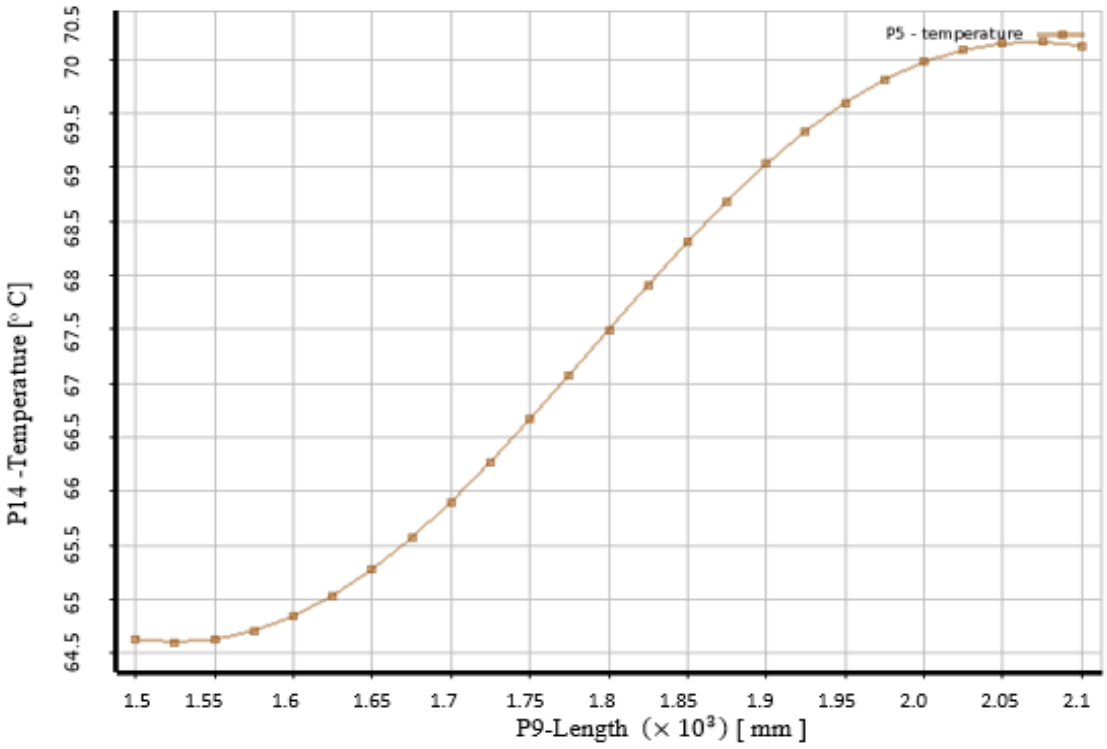

Figure 4.13: Temperature Response to Change in Collector Length

From the temperature response to change in collector length chart, a sharp rise in temperature was observed from a collector length of 1600 mm to 2000 mm where the curve began to flatten. Figure 4.14 shows how the average temperature in the storage tank responds to changes in the collector tube diameter. It was observed from the temperature- diameter response chart that the collector tube diameter greatly affected the average water temperature in the storage tank.

Changes in the collector tilt angle, the collector tube length and the collector tube diameter were found to have appreciable influence on the flow velocity in the system. The collector tilt angle had a marginal influence on the average temperature in the storage tank as presented in Figure 4.15. However, variations in the flow velocity was observed as the tilt angle was varied from 10 to 50 degrees.

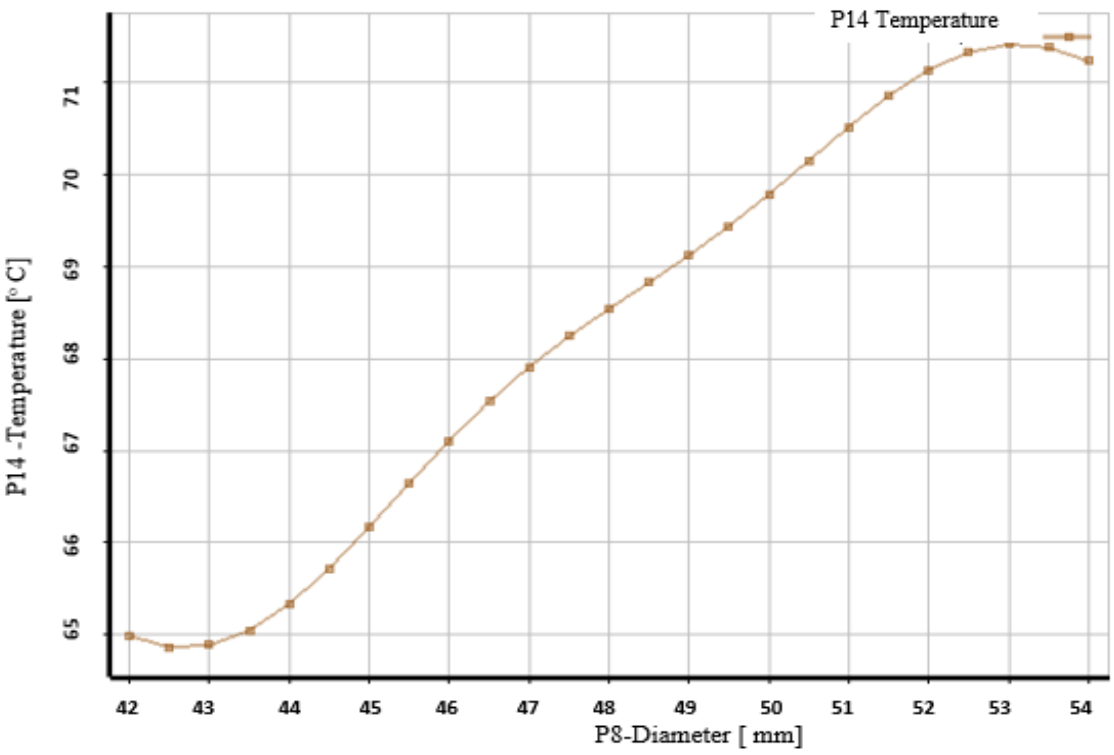

Figure 4.14: Temperature Response to Change in Collector Diameter

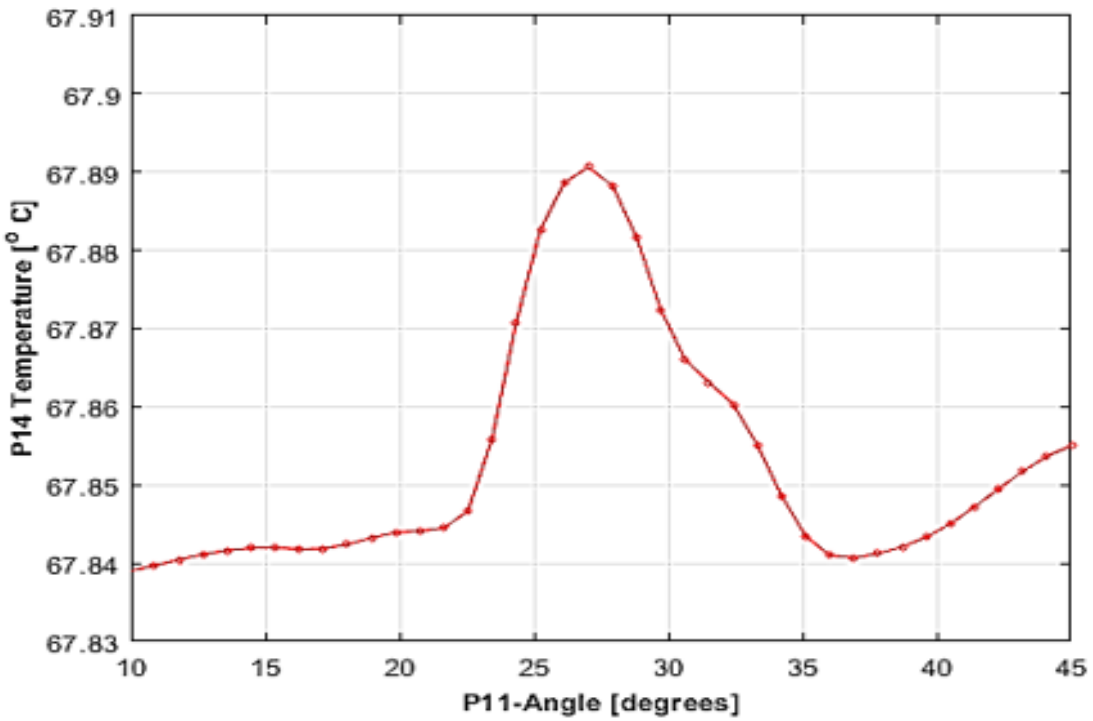

Figure 4.15: Temperature Response to Change in Collector Tilt Angle

These three design variables were optimized to improve the performance of the water in glass evacuated tube solar water heater using ANSYS design exploration. From the optimization data, the optimum collector tube length was found to be 2000 mm taking into account installation space requirements and ease of system transportation. The optimum collector diameter was found to be 50 mm and the optimum collector tilt angle was found to be 28 degrees.

The water outlet temperature and the average flow velocity from the CFD simulation were 67.9 ^{o} C and 0.00017 ms^{-1} respectively whereas the optimized CFD model recorded water outlet temperature of 72.0 ^{o} C and an average flow velocity of 0.00019 ms^{-1}. The optimized design of the WG-ETSWH enhanced the outlet temperature of the water in the storage tank by 6.0 % and the average flow velocity of water in the system by 11.8 %.

Figure 4.16 and Figure 4.17 shows the temperature and velocity distribution of the optimized CFD model.

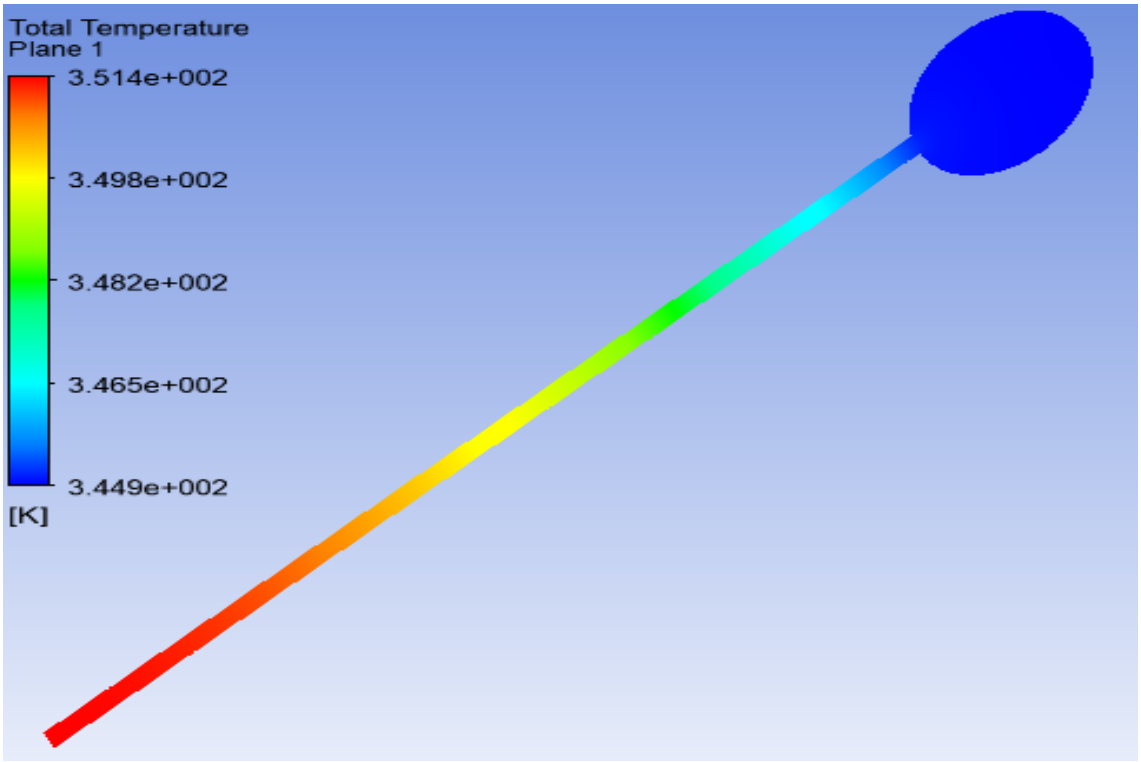

Figure 4.16: Temperature Distribution in the Optimized CFD Model

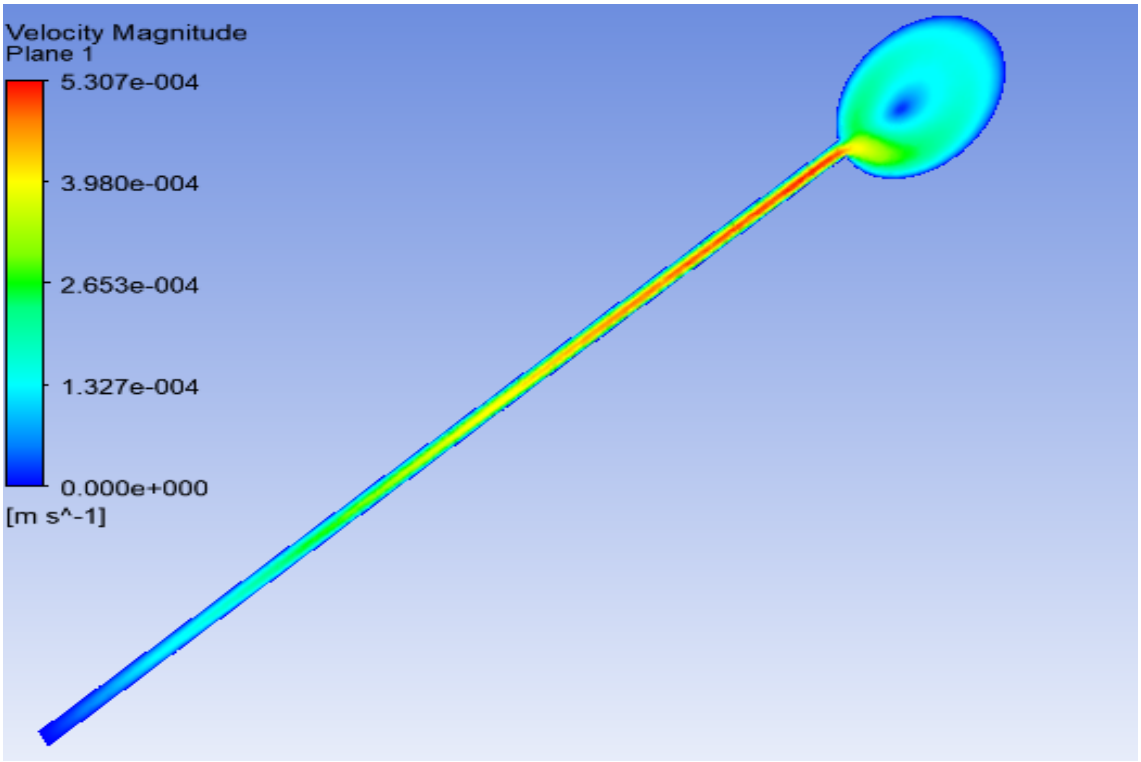

Figure 4.17: Velocity Distribution in the Optimized CFD Model

CHAPTER FIVE

CONCLUSION AND RECOMMENDATIONS

5.1 Conclusion

In this research study, the thermal performance of water in glass evacuated tube solar water heater was investigated. An experimental study on the performance of water in glass evacuated tube solar water heater was conducted under the climatic conditions in Kenya. A CFD model was developed according to the specifications of the experimental setup and validated with experimental data.

The validated CFD model was used to study the influence of geometric variables including the collector tilt angle, collector tube diameter and the collector tube length on the performance of the system. These geometric variables were optimized using ANSYS design exploration package to improve the performance of water in glass evacuated solar water heater. The following conclusions were made from the findings of this research study;

- The final outlet temperature of the water in glass evacuated tube solar water heater was found to be ranged from 55 ^{o} C to 70 ^{o} C given an initial temperature of 25 ^{o} C for a typical whole day heat collection. The daily efficiency of the water in glass evacuated tube solar water heater under the

climatic conditions in Kenya ranges from 58% to 65%. It can be concluded that water in glass evacuated tube solar water heater is highly suitable for domestic water heating applications in Kenya.

- The length of the collector tube was found to have a significant effect on the temperature of water in the storage tank and the velocity distribution in the system. Increasing the collector length greatly enhances the performance of the WG-ESTWH. However, the sizing of the collector length must take into account installation space and ease of transportation. It can be concluded that the optimum length of the collector tube is 2000 mm.

- The Collector tilt angle has marginal effect on the temperature distribution within the storage tank. However, the influence of the collector tilt angle was seen in the water circulation rate. The average flow velocity for lower tilt angles were better than for higher tilt angles. From the temperature and velocity contours for the various tilt angles, it can be concluded that the optimum tilt angle is 28 degrees.

- The diameter of the collector tube of the WG-ETSWH affects the solar heat flux, the flow rate of water and the temperature distribution in the storage tank. Increasing the diameter of the collector tube increases the heat gain of the system. This led to the conclusion that the diameter of the collector tube has a significant effect on the performance of the water in glass evacuated tube solar water heater.

5.2 Recommendations

The research work aimed to improve the thermal performance of water in glass evacuated tube solar water heater. To further improve the performance of WG-ETSWH and enhance its utilization , the following recommendations are highlighted for further studies.

- A major deviation in water temperature was seen at the portions below the tube opening and the portions above the tube opening in the storage tank. This was as a result of the angle at which the collector tubes were inserted into the storage tank. Further research studies are needed to establish the conditions that will help to overcome this challenge.

- The absorptivity, reflectivity and transmissivity of the collector materials affects the rate of absorption of the solar irradiation. Further research studies on the optical properties of the materials used for the collector are required to improve the performance of WG-ETSWH.

- The number of collector tubes may influence the performance of the water in glass evacuated tube solar water heater. More research is required to establish the influence of the number of collector tubes on the performance of the solar water heater.

- The collector tube length and diameter were found to have a significant effect on the performance of the system. However, increasing the collector tube length and diameter may affect the cost of the WG-ETSWH. Further research work is needed to establish how increasing the collector tube length and diameter may affect the current cost of the system.

- The solar radiation absorption rate can be enhanced by the use of a solar tracker system. Further research can be done in this area to improve the solar energy gain by the collector.

REFERENCES

Alanne, K., & Saari, A. (2006). Distributed energy generation and sustainable development. *Renewable and Sustainable Energy Reviews*, *10*, 539–558.

Alfaro-Ayala, J. A., Martínez-Rodríguez, G., Picón-Núñez, M., Uribe-Ramírez, A. R., & Gallegos-Muñoz, A. (2015). Numerical study of a low temperature water-in-glass evacuated tube solar collector. *Energy Conversion and Management*, *94*, 472–481.

Ali Omer Ali, A. (2019). *Optimization of thermal performance of a flat plate solar collector using numerical simulation in sahara regions* (Masters). Pan African University Institute for Baisc Sciences, Technology and Innovation.

Antony, J. (2014). *Design of experiments for engineers and scientists* (second ed.). USA: Elsevier.

Armaroli, N., & Balzani, V. (2007). The future of energy supply : challenges and opportunities. *Renewable Energies*, 52–66.

Ayompe, L. M., & Duffy, A. (2013). Thermal performance analysis of a solar water heating system with heat pipe evacuated tube collector using data from a field trial. *Solar Energy*, *90*, 17–28.

Ayompe, L. M., Duffy, A., McCormack, S. J., & Conlon, M. (2011). Validated TRNSYS model for forced circulation solar water heating systems with flat plate and heat pipe evacuated tube collectors. *Applied Thermal Engineering*, *31*(8-9), 1536–1542.

Beňo, P., Kozak, D., & Konjatić, P. (2014). Optimization of thin-walled construction in CAE system ANSYS. *Technical gazette*, *3651*(ISSN 1330-3651), 1051–1056.

Bevington, R., & Robinson, D. K. (2003). *Data reduction and error analysis for the physical sciences* (3rd ed.). New York: McGraw-Hill.

Bracamonte, J., Parada, J., Dimas, J., & Baritto, M. (2015). Effect of the collector tilt angle on thermal efficiency and stratification of passive water in glass evacuated tube solar water heater. *Applied Energy*, *155*, 648–659.

Budihardjo, I., & Morrison, G. L. (2009). Performance of water-in-glass evacuated tube solar water heaters. *Solar Energy*, *83*(1), 49–56.

Budihardjo, I., Morrison, G. L., & Behnia, M. (2003). Development of TRNSYS models for predicting the performance of water-in-glass evacuated tube solar water heaters in Australia. In *School of mechanical and manufacturing engineering* (pp. 1–10).

Budihardjo, I., Morrison, G. L., & Behnia, M. (2007). Natural circulation flow through water-in-glass evacuated tube solar collectors. *Solar Energy*, *81*(12), 1460–1472.

Dindi, A. (2013). The impact of the rapid expansion of universities on their neighbourhood development; a case study of JKUAT, Juja campus..

Division Goodfellow Ceramics and Glass. (2008). Borosilicate glass - properties of borosilicate glass (Pyrex/Duran). *Available at : www.azom.com/article.aspx?ArticleID=4765 [Accessed: 20th March,2021]*.

Energy Analyis. (2019). *BP statistical review of world energy* (Tech. Rep.).

Energy Analyis. (2020). *BP statistical review of world energy* (Tech. Rep.).

Engineering Toolbox. (2007). Polyurethane insulation [online]. *Available at : https://www.engineeringtoolbox.com/polyurethane-insulation-k-values-d_1174.html [Accessed: 10th June, 2021]..*

ESCO. (2015). Flat plate solar water heater – solar collectors. *Available at : https://www.aspessolarproducts.com/sol [Accessed : 1st April, 2021]*.

Fluent, A. (2018). *ANSYS fluent user guide.* U.S.A: ANSYS Inc.

Gao, Y., Zhang, Q., Fan, R., Lin, X., & Yu, Y. (2013). Effects of thermal mass and flow rate on forced-circulation solar hot-water system: Comparison of water-in-glass and U-pipe evacuated-tube solar collectors. *Solar Energy*, *98*(PC), 290–301.

Global Alliance for Buildings and Construction. (2019). *International energy agency and the united nations (2019): 2019 Global Status Report for Buildings and Construction:Towards a zero-emission, efficient and resilient buildings and construction sector.* (Tech. Rep.).

Hayek, M. (2009). Investigation of evacuated-tube solar collectors performance using computational fluid dynamics. In *2009 international conference on advances in computational tools for engineering applications, actea 2009* (pp. 240–244).

Hayek, M., Assaf, J., & Lteif, W. (2011). Experimental investigation of the performance of evacuated-tube solar collectors under Eastern mediterranean climatic conditions. *Energy Procedia*, *6*, 618–626.

He, Y., Jamieson, C., Jeary, A., & Wang, J. (2008). Effect of computation domain on simulation of small compartment fires. , 1365–1376.

Kalogirou, S. A. (2004). Environmental benefits of domestic solar energy systems. *Energy Conversion and Management*, *45*(18-19), 3075–3092.

Kamau, D. W. (2013). An analysis of household choices in major cities in Kenya. *Journal of Chemical Information and Modeling*, *53*(9), 1689–1699.

Kannan, N., & Vakeesan, D. (2016). Solar energy for future world : - A review. *Renewable and Sustainable Energy Reviews*, *62*, 1092–1105.

Kyekyere, E., Ndiritu, H., Hawi, M., & Mwambe, P. (2021). Performance of water in glass evacuated tube solar water heater under Kenya climatic condition. *Computational Water, Energy, and Environmental Engineering*, *10*, 37–48.

Lee, D. W., & Sharma, A. (2007). Thermal performances of the active and passive water heating systems based on annual operation. *Solar Energy*, *81*(2), 207–215.

Liu, Z., Li, H., Liu, K., Yu, H., & Cheng, K. (2017). Design of high-performance water-in-glass evacuated tube solar water heaters by a high-throughput screening based on machine learning: A combined modeling and experimental study. *Solar Energy*, *142*, 61–67.

Ma, L., Lu, Z., Zhang, J., & Liang, R. (2010). Thermal performance analysis of the glass evacuated tube solar collector with U-tube. *Building and Environment*, *45*(9), 1959–1967.

Menon, A. (2005). *Structural optimization using ANSYS and regulated multi-quadric response surface model* (Masters). The University of Texas.

Mohammadkarim, A., Kasaeian, A., & Kaabinejadian, A. (2014). Performance investigation of solar evacuated tube collector using TRNSYS in Tehran. *International Journal of Renewable Energy Research*, *4*(2), 497–503.

Momanyi, A. B. (2015). *Solar water heating in urban housing: A study of factors affecting adoption among households in Nairobi* (Master's thesis). University of Nairobi.

Morrison, G. L., Budihardjo, I., & Behnia, M. (2004). Water-in-glass evacuated tube solar water heaters. *Solar Energy*, *76*(1-3), 135–140.

Morrison, G. L., Budihardjo, I., & Behnia, M. (2005). Measurement and simulation of flow rate in a water-in-glass evacuated tube solar water heater. *Solar Energy*, *78*(2), 257–267.

Ng'ethe, J. (2015). *Performance optimisation of a thermosyphon flat plate solar water heater* (Master's thesis). Jomo Kenyatta University of Agriculture and Technology.

Panwar, N. L., Kaushik, S. C., & Kothari, S. (2011). Role of renewable energy sources in environmental protection : A review. *Renewable and Sustainable Energy Reviews*, *15*(3), 1513–1524.

Rao, S. S. (2009). *Engineering optimization: Theory and practice* (Fourth ed.). Hoboken, New Jersey: John Wiley & Sons, Inc.

REN21. (2019). *Renewables 2019 global status report* (Tech. Rep.). Paris: REN21 Secretariat.

Sato, A. I., Scalon, V. L., & Padilha, A. (2012). Numerical analysis of a modified evacuated tubes solar collector. In *International conference on renewable energies and power quality* (Vol. 1, pp. 384–389). Santiago de Compostela (Spain).

Shah, L. J., & Furbo, S. (2007). Theoretical flow investigations of an all glass evacuated tubular collector. *Solar Energy*, *81*(6), 822–828.

Stryi-Hipp, G., Weiss, W., D. Mugnier, , & Dias, P. (2012). Strategic research priorities for solar thermal technology. *European Technology Platform on Re- newable Heating and Cooling (Belgium)*.

Suresh, K., & Regalla, S. P. (2014). Effect of mesh parameters in finite element simulation of single point incremental sheet forming process. *Procedia Materials Science*, *6*(Icmpc), 376–382.

Tang, R., Gao, W., Yu, Y., & Chen, H. (2009). Optimal tilt-angles of all-glass evacuated tube solar collectors. *Energy*, *34*(9), 1387–1395.

Tang, R., Yang, Y., & Gao, W. (2011). Comparative studies on thermal performance of water-in-glass evacuated tube solar water heaters with different collector tilt-angles. *Solar Energy*, *85*(7), 1381–1389.

Taylor, R. J. (1997). *An introduction to error analysis: The study of uncertainties in physical measurements* (2nd ed.). sausalito, California.

Tiwari, G., Shyam, & Tiwari, A. (2018). *Handbook of solar energy : Theory, analysis and applications* (U. Muhammad H. Rashid, Pensacola, Ed.). Singapore: Springer.

Veeraboina, P., & Ratnam, G. Y. (2012). Analysis of the opportunities and challenges of solar water heating system (SWHS) in India : Estimates from the energy audit surveys & review. *Renewable and Sustainable Energy Reviews*, *16*(1), 668–676.

Versteeg, H. K., & Malalasekera, W. (2007). *An introduction to computational fluid dynamics* (Second ed.). Berlin, Heidelberg: Pearson Education Limited.

Yao, K., Li, T., Tao, H., Wei, J., & Feng, K. (2015). Performance evaluation of all-glass evacuated tube solar water heater with twist tape inserts using CFD. *Energy Procedia*, *70*, 332–339.

Zhang, X., You, S., Xu, W., Wang, M., He, T., & Zheng, X. (2014). Experimental investigation of the higher coefficient of thermal performance for water-in-glass evacuated tube solar water heaters in China. *Energy Conversion and Management*, *78*, 386–392.

APPENDICES

Appendix 1: Measuring Devices

Solar Power Meter

Digital Solar Power Meter was used to measure the solar irradiation falling on the surface of he collector tube. It measures solar irradiation in W/m^2 with a response time of 0.25 seconds. Its range of measurement is between 0 to 2000 W/m^2. Figure A.1 shows the Solar Power Meter used for measuring the solar irradiation.

Figure A.1: Digital Solar Power Meter for Measuring Solar Irradiation

Weather Station WH2C Thermo-Hygrometer

Weather Station Thermo-Hygrometer was used to measure the atmospheric temperature. The instrument was calibrated to ensure its accuracy. The instrument measures wireless outdoor temperatures within the range of -40 to 65 ^{o}C and an indoor temperatures ranged from 0-40 ^{o}C. Its transmission range up to 300 feet open air. Figure A.2 shows the Weather Station Thermo-Hygrometer (Receiver) used for measuring the atmospheric temperature.

Figure A.2: Weather Station for Measuring Atmospheric Temperature

TNA 110 Thermometer

The inlet and outlet temperatures were measured using TNA 110 digital thermometer. To instrument was calibrated to ensure the accuracy of the measurements. The TNA 110 thermometer can measure temperatures within the range of -65 to 1000 ^{o}C with a precision of $\pm$ 1 ^{o}C. Figure A.3 shows the TNA 110 Thermometer used for measuring the inlet and outlet temperatures.

Figure A.3: TNA Thermometer for Measuring Temperature of Water

Appendix 2: Performance of WG-ETSWH

Table A.1 shows the daily irradiation, the daily heat gain, the average atmospheric temperature (T_a) and daily thermal efficiency of the system for four different days.

Table A.1: Performance of Water in Glass Evacuated Tube SWH

Date	**G(MJm^{-2})**	$\dot{Q}$**(MJ)**	$T_a(^o\mathbf{C})$	$T_{in}(^o\mathbf{C})$	$T_{out}(^o\mathbf{C})$	η_d
26th January, 2021	20.12	37.62	27.4	28	64	0.623
28th January, 2021	21.00	42.85	28.6	27	68	0.622
29th January, 2021	20.41	41.80	28.7	29	69	0.624
2nd February, 2021	20.24	37.60	29.0	28	64	0.620

Appendix 3: Model Validation

Figure A.4 shows the graphical representation of the comparison of simulated results and experimental results.

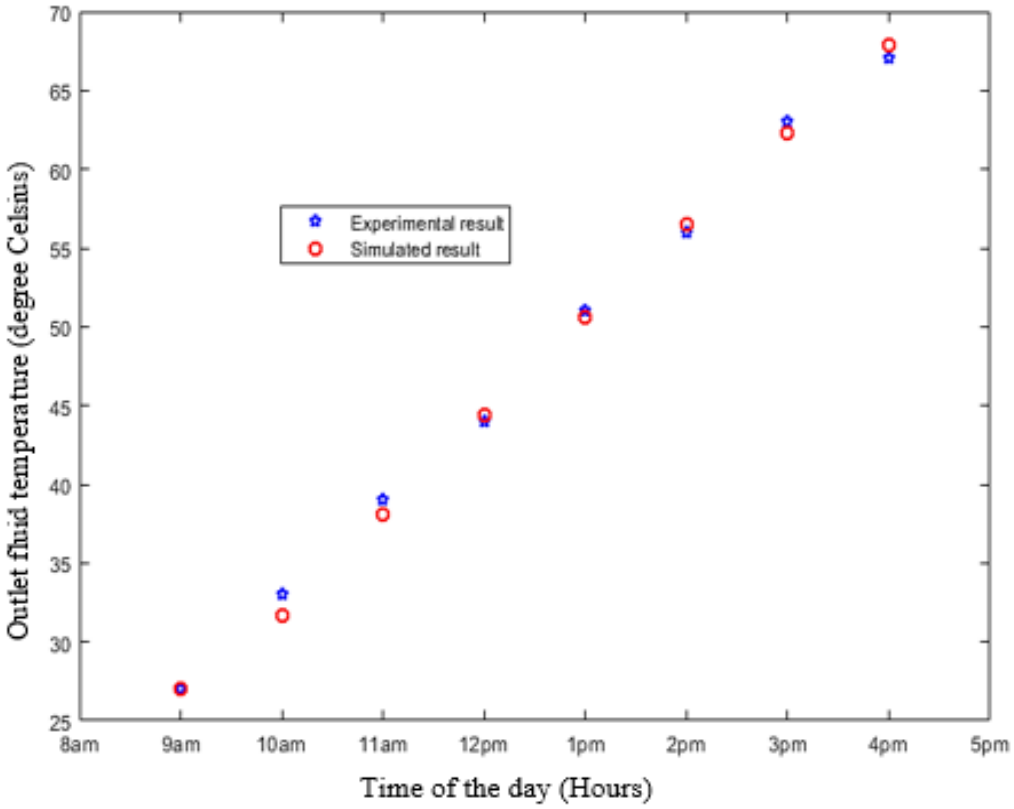

Figure A.4: Comparison of Experimental and Simulation Results

Appendix 4: Velocity and Temperature Contours

Figure A.5 and Figure A.6 shows the temperature and velocity distribution for collector length of 1600 mm, collector diameter of 47 mm and a tilt angle of 23 degrees .

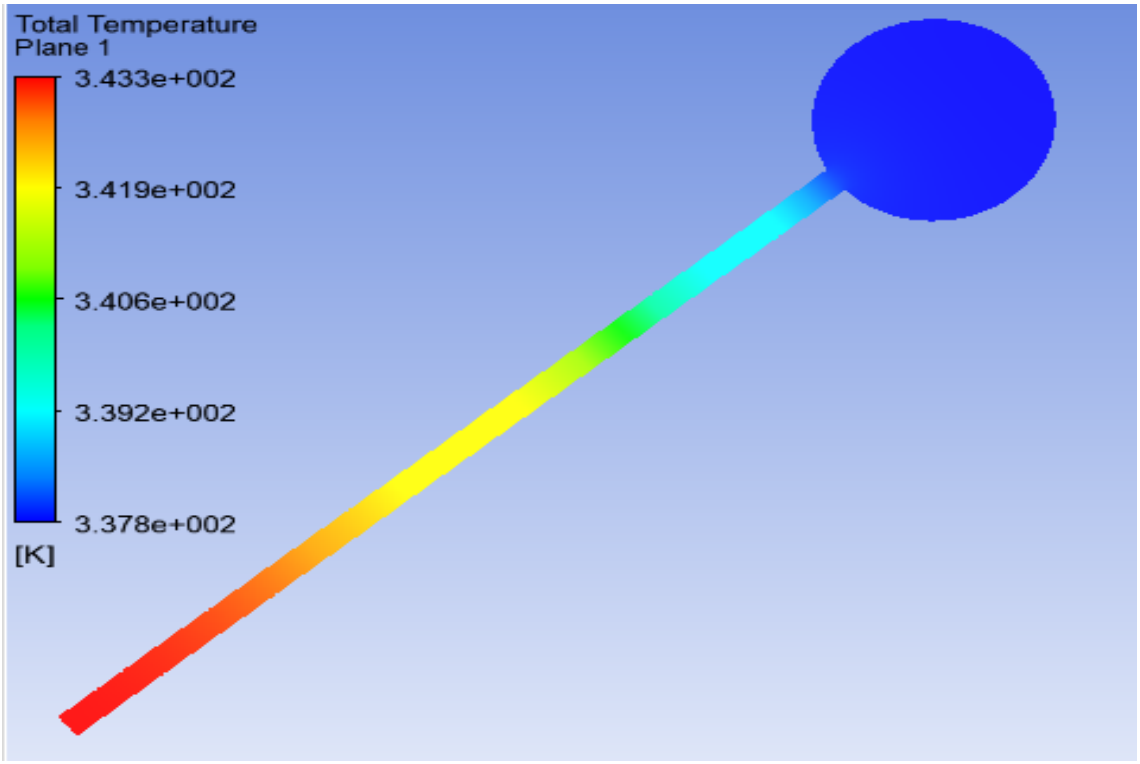

Figure A.5: Temperature Distribution for Collector Length of 1600mm

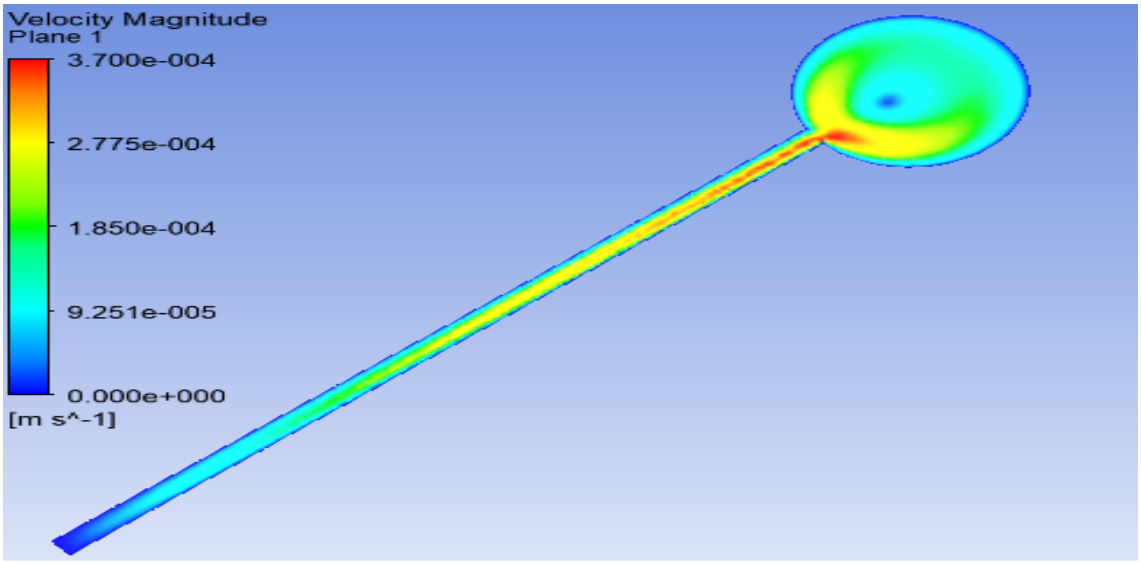

Figure A.6: Velocity Distribution for Collector Length of 1600mm

Figure A.7 shows the temperature distribution for collector length of 1800 mm, diameter of 52 and a tilt angle of 23 degrees.

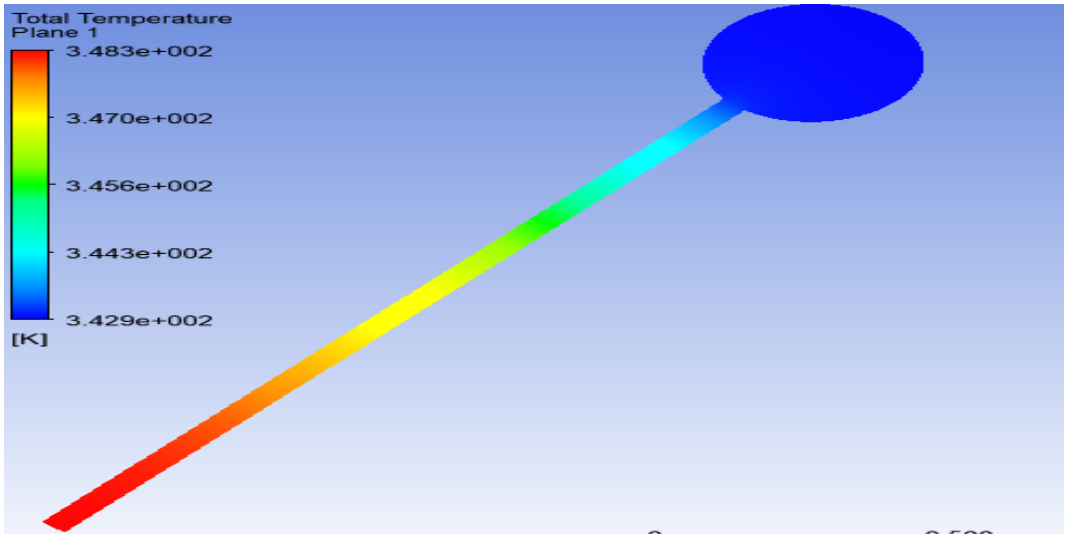

Figure A.7: Temperature Distribution for Collector Diameter of 52 mm